


Review

# Research Progress on Effects of Antifreeze Components, Nanoparticles and Pre-Curing on the Properties of Low-Temperature Curing Materials

Xianhua Yao <sup>1,\*</sup> , Mingduo Wan <sup>1</sup>, Yongsheng Zhu <sup>2</sup>, Lihua Niu <sup>1</sup>, Xiaoxiang Ji <sup>3</sup>, Shengqiang Chen <sup>4</sup>, Wei He <sup>1</sup> and Linyan Han <sup>1</sup>

<sup>1</sup> School of Civil Engineering and Communication, North China University of Water Resources and Electric Power, Zhengzhou 450045, China; wmd991222@163.com (M.W.); niulihua@ncwu.edu.cn (L.N.); hewei@ncwu.edu.cn (W.H.); 15093433832@163.com (L.H.)

<sup>2</sup> Northeast Branch China Construction Eighth Engineering Division Co., Ltd., Dalian 116000, China; z18339157108@163.com

<sup>3</sup> School of Highway, Henan College of Transportation, Zhengzhou 451450, China; docling@126.com

<sup>4</sup> Henan Building Materials Research and Design Institute Co., Ltd., Zhengzhou 450018, China; csq737@163.com

\* Correspondence: yaoxianhua@ncwu.edu.cn

**Abstract:** There are long periods of winter construction in China's eastern and western Alpine regions. The decreased construction temperature adversely affects the workability, mechanical properties, and durability of cement-based materials and alkali-activated materials. Under low-temperature curing conditions, the hydration reaction of these materials slows down, resulting in limited strength development and reduced durability. In response to this problem, researchers have summarized three measures to improve performance: the use of anti-freezing components, nanoparticles, and pre-curing. The effects of anti-freezing components on the mechanical properties and micro-mechanism changes of Portland cement, sulphoaluminate cement, magnesium phosphate cement-based materials, and alkali-activated cementitious materials are organized. Additionally, the improvement of macro-micro properties in cement-based materials through mineral admixtures, nanoparticles, and hydrated calcium silicate seeds is summarized. The influence of pre-curing on the mechanical properties of cement-based materials is analyzed, focusing on the relationship between pre-curing time and the critical strength of frost resistance. Finally, existing research challenges are summarized, and future research directions are proposed, providing valuable references for the further development of materials and engineering applications.

**Keywords:** low-temperature curing; antifreeze components; nanoparticles; pre-curing; mechanical properties



Academic Editor: Duc-Kien Thai

Received: 9 December 2024

Revised: 4 January 2025

Accepted: 7 January 2025

Published: 14 January 2025

**Citation:** Yao, X.; Wan, M.; Zhu, Y.; Niu, L.; Ji, X.; Chen, S.; He, W.; Han, L. Research Progress on Effects of Antifreeze Components, Nanoparticles and Pre-Curing on the Properties of Low-Temperature Curing Materials. *Buildings* **2025**, *15*, 223. <https://doi.org/10.3390/buildings15020223>

**Copyright:** © 2025 by the authors. Licensee MDPI, Basel, Switzerland. This article is an open access article distributed under the terms and conditions of the Creative Commons Attribution (CC BY) license (<https://creativecommons.org/licenses/by/4.0/>).

## 1. Introduction

China has a vast territory and a large north–south span, resulting in complex and diverse climate types. After pouring concrete in high-cold and high-altitude areas, it is cured under negative temperatures (−30 °C to 0 °C). Under this condition, the hydration process of concrete materials can be affected or even suspended. The mechanical properties and durability of concrete materials will be greatly reduced if no measures are taken [1,2], and this further affects the safe operation of the building. With the further growth of economic development and engineering construction demand, studying the construction of winter negative temperatures in alpine and high-altitude areas is of great practical significance, as it can accelerate the construction of basic projects in these areas [3–5].

Compared to standard and high-temperature curing conditions, the initial hydration process of the material is hindered, slowed, or even aborted under low-temperature curing, especially under negative-temperature curing. The coagulation time is delayed, allowing less time for the dissolved ions to diffuse before the hydrate precipitates, resulting in a lower density of C-S-H [1]. The microstructure of early cement-based materials is not fully developed, leading to early failure and accelerating the deterioration of concrete strength in the later stage. Additionally, the cement-based material exhibits non-uniformity. The temperature stress generated during the cooling process will act on its internal structure, and the frost heave damage will cause structural damage [6,7], thereby affecting later durability. Compared with Portland cement-based materials under negative-temperature conditions, the alkali-activated cementitious material solution contains abundant free ions, which can reduce the freezing point of the solution in the mixture. It is theoretically feasible to prepare alkali-activated cementitious materials at negative temperatures, which has the potential for water hardening at negative temperatures [8]. With the further growth of the demand for infrastructure and traffic engineering in high-cold and high-altitude areas, some scholars have also begun to study the mechanical properties of new cementitious materials at negative temperatures to apply them in infrastructure construction or as repair materials in cold weather conditions [9–11].

Currently, two methods are utilized to prevent the frost damage of cement-based materials under low-temperature conditions in winter. The first category mainly includes the implementation of thermal insulation measures, the use of heating systems, and protective coverings such as the steam heating method and warm shed method [12,13]. Pre-curing in advance allows the material to form an early structure [14] and achieve its critical strength for frost resistance [15,16]. The second category is based on the use of appropriate materials [9,17,18] and admixtures such as early strength agents, antifreeze, nanoparticles, and fibers [19–25] to improve the negative-temperature mechanical properties of the material.

In this study, the experimental study of cement-based materials under low-temperature curing is organized. On the one hand, the effects of antifreeze components and nanoparticles on the hydration process and mechanical properties of different cement-based materials under low-temperature curing are summarized, and the changes in microstructure and strength properties are analyzed. On the other hand, the pre-curing method is used in winter construction. The pre-curing time varies at different temperatures. In the specification of JC/T475-2004 [26], the pre-curing times of 6, 5, and 4 h were used for concrete with antifreeze at  $-5$ ,  $-10$ , and  $-15$  °C, respectively. However, this provision is too general and not refined to different low-temperature curing methods [27] and different degradation degrees [28,29]. Based on the above, the research status of the influence of different pre-curing times on the low-temperature mechanical properties of different materials and the relationship between pre-curing time and the critical strength of frost resistance are sorted out for reference in winter construction.

## **2. Effect of Antifreeze Components on the Mechanical Properties and Microstructure of Different Cement-Based Materials and Alkali-Activated Materials Under Low-Temperature Curing**

Portland cement has been widely used in all kinds of buildings since its invention in 1824 [5]. At present, the development system is well-established, with numerous scholars having already begun to study the performance changes of Portland cement-based materials under different temperature conditions [30–32]. The term “first series of cement” generally refers to Portland cement products, whereas the sulfoaluminate cement developed around the 1970s is considered the second series [33]. Due to its advantageous characteristics, including low-energy consumption, early strength, high frost resistance,

corrosion resistance, and high impermeability, a series of cement-based materials has been derived. These materials are utilized in winter construction projects, emergency repairs, and rapid construction projects [33,34]. Subsequently, at the end of the twentieth century, research on magnesium phosphate cement conducted in China revealed that despite its rapid reaction and short operable time before setting, the introduction of retarding components has enabled its effective use in rapid repair projects [35,36]. At the same time, the research on alkali-activated cementitious materials has evolved, utilizing widely available solid waste as a precursor and a chemical reagent to prepare an alkaline solution as an activator to adjust its performance. These materials are noted for their controllability and superior mechanical properties. Therefore, it is called a substitute for Portland cement [37,38]. Under the condition of low temperatures in winter, the hydration of cement-based materials is slow or stagnant. The incorporation of various antifreeze components reduces frost heave damage, promotes early hydration, and improves mechanical properties. The mechanism of antifreeze includes ice crystal distortion theory, Raoult's law, liquid–ash ratio equilibrium theory, and maturity theory. The incorporation of various anti-freezing components can be attributed to the method of reducing freezing points, changing crystal formation, employing early strength anti-freezing techniques, and integrating superplasticizers [20,39–42]. The rational use of antifreeze is an effective measure to prevent early failures and enhance the frost resistance of concrete [43,44]. Consequently, the influence of incorporating different antifreeze components on the properties of these materials under low-temperature curing conditions is categorized into four groups: ordinary Portland cementitious materials, newly developed cement-based materials with superior properties such as sulfoaluminate cement and magnesium phosphate cement, and alkali-activated cementitious materials with promising development potential.

## 2.1. Portland Cement

As the most widely used cementitious material, the performance of ordinary Portland cement-based materials under normal temperature curing has been a concern for scholars [45–48]. In order to speed up the hydration process of cement-based materials at low temperatures and improve mechanical properties, scholars have tried to add various antifreeze components such as inorganic salts, organic salts, and admixtures.

### 2.1.1. Mechanical Properties

Composite antifreeze is a mixed solution containing antifreeze, early strength, air entrainment, and water reduction components. It has been used by scholars in concrete materials to improve the deterioration of its negative-temperature performance [49–51]. Subsequently, experimental studies on the mechanical properties of different single components mixed with Portland cement-based materials are also carried out successively, among which the properties of ethylene glycol, calcium chloride, calcium nitrate, and sodium nitrite incorporated into concrete are studied more (Table 1). The effect of different dosages of ethylene glycol is not obvious under the condition of early negative temperature, but after being transferred to positive temperature curing, the later strength of concrete increases with the increase of dosage. When the temperature is lower ( $-10\text{ }^{\circ}\text{C}$ ,  $-15\text{ }^{\circ}\text{C}$ ), the incorporation of ethylene glycol can play a relatively good antifreeze effect under the maintenance of negative temperature to positive temperature [52]. Increase the rate of compressive strength (IRCS) of ordinary cement-based materials with different anti-freezing ingredients (Table 1).

**Table 1.** Effect of antifreeze components on compressive strength of ordinary cement-based materials.

Serial Number	Curing Temperature (°C)	Antifreeze Component	Optimum Content (%)	Age (d)	IRCS (%)	Refs.
1	−20	Antifreeze early strength water reducer	5	−7 + 56	112	[49]
2	−15	CaCl <sub>2</sub>	7	−7 + 28	72	[52]
3	−15	C <sub>2</sub> H <sub>6</sub> O <sub>2</sub>	1.5	−7 + 56	70	[53]
4	−15 ± 0.5	NaNO <sub>2</sub>	2	−7 + 28	100	[54]
5	−15	Ca(NO <sub>3</sub> ) <sub>2</sub>	6	−28 + 28	263	[55]
6	−10	CO(NH <sub>2</sub> ) <sub>2</sub>	6	−14 + 28	45	[56]
7	−10	CaCl <sub>2</sub>	7	−7 + 28	49	[57]
8	−5	K <sub>2</sub> CO <sub>3</sub>	5	−28	40	[58]
9	−20	NaNO <sub>2</sub>	5	−7 + 28	−36	[59]
10	−5	Ca(NO <sub>3</sub> ) <sub>2</sub>	1	−28	92	[60]
11	−10	Ca(NO <sub>3</sub> ) <sub>2</sub> + CO(NH <sub>2</sub> ) <sub>2</sub>	4.5 + 4.5	−90	208	[61]
12	−10	Ca(NO <sub>3</sub> ) <sub>2</sub> + CNNaS	8 + 1.5	−28 + 28	427	[62]
13	−15	Non-chloride salt + C <sub>6</sub> H <sub>15</sub> NO <sub>3</sub> + C <sub>2</sub> H <sub>6</sub> O <sub>2</sub>	20 + 1 + 7.5	−7 + 56	26	[50]

Note: The ‘−’ in the compressive strength increase rate indicates that the strength decreases; in the age, ‘−’ represents negative-temperature curing, ‘+’ represents positive temperature curing; the increase rate of compressive strength is based on the middle age of the table.

For spontaneous combustion coal gangue concrete, the strength of coal gangue concrete is also improved with the increase of dosage under the condition of negative temperature to positive temperature [57]. Under the curing conditions of −5 °C, −10 °C, and −15 °C, the four anti-freezing components of calcium chloride, calcium nitrate, calcium nitrite, and ethylene glycol can all play a good anti-freezing effect. The order of antifreeze effect is calcium chloride > calcium nitrate > ethylene glycol > calcium nitrite [52,57]. At −5 °C and −10 °C, the positive effect of urea antifreeze is more obvious, but at −15 °C and −20 °C, compared with the specimens without antifreeze, the expected effect is not achieved [56]. However, the compressive strength and ultrasonic wave velocity of 7 and 28 days were very low when 4.5% urea + 4.5% calcium nitrate was mixed as an antifreeze component and cured at −15 and −20 °C. Especially in the sample containing 9% urea, the high content of urea is not suitable for the negative-temperature freezing injury of concrete. However, with the increase of curing time, the compressive strength and ultrasonic wave velocity of the sample of the 4.5% urea + 4.5% calcium nitrate combination increased. Under outdoor winter conditions, the 28-day compressive strength of the sample with 4.5% calcium nitrate and 4.5% urea was increased by about 108% and 82%, respectively, compared with the control sample under the same conditions [62]. Adding 5% NaNO<sub>2</sub>, as an antifreeze agent can accelerate hydration and lower the freezing point in the early stages. However, in a −20 °C environment, during the freeze–thaw process, the early-established network of hydration products may be damaged by the freeze–thaw stresses [59]. At −15 °C, with a 2% dosage of NaNO<sub>2</sub> the IRCS reached 100%, demonstrating excellent performance [54]. At −10 °C, (Ca(NO<sub>3</sub>)<sub>2</sub> + CO(NH<sub>2</sub>)<sub>2</sub>, dosage of 4.5 + 4.5%) achieved an IRCS as high as 208%, indicating that an appropriate dosage of antifreeze can significantly enhance the compressive strength of concrete [61]. In the short-term curing period (e.g., −7 days), the performance was relatively low. However, with the increase in curing time at room temperature (28 days), the strength gradually recovered and even exceeded the normal value, reaching 263% [55].

In order to reduce the freezing point of the solution and reduce the amount of frozen water, the incorporation of various antifreeze components was selected. However, when the antifreeze cannot ensure that the water inside the concrete remains in the liquid phase state, the addition of most of the inorganic antifreeze in the concrete will reduce the frost heave deformation of the concrete, but it will increase the residual deformation and

form a loose structure, and finally increase the degree of frost damage of the concrete to varying degrees. It can be seen that not all the incorporation of antifreeze components can produce beneficial effects, and an appropriate dosage is needed to maintain the liquid phase equilibrium, thereby improving frost resistance [59]. At present, ordinary portland cement-based materials are still the mainstream cementitious materials. The type and dosage of antifreeze components need to be combined with factors such as performance improvement effect, field working conditions, and economic principles.

### 2.1.2. Microscopic Mechanism

Negative temperature curing leads to an early loose structure of cement paste. The lower the curing temperature, the larger the pore size of the cement paste. As shown in Figure 1. The micropore volume of <20 nm and 20–100 nm decreased significantly, the macropore volume increased sharply, and the damage to the internal pore structure of the sample was more serious due to negative-temperature frost damage [59,63]. The early strength of concrete without antifreeze at  $-10^{\circ}\text{C}$  is very low, and the antifreeze component can effectively reduce the microcracks caused by early negative-temperature curing of concrete [64].

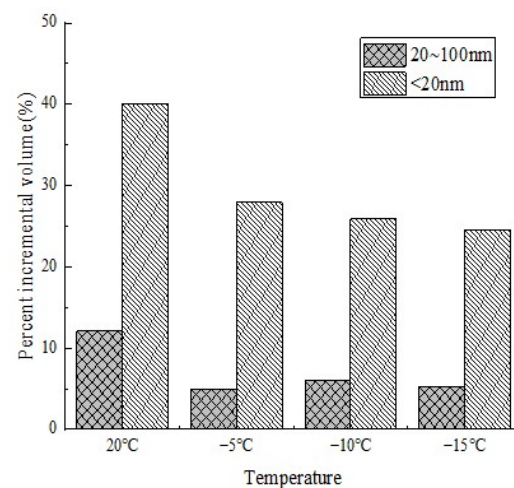


**Figure 1.** Effect of curing temperature on the pore structure of cement paste at 7 days [63].

The hydration process is seriously hindered or stagnant under negative-temperature curing, and the heat of cement hydration is more favorable to the concrete project constructed in winter, which can improve early strength. The hydration heat test can directly reflect the hydration heat release of the material at a negative temperature and whether the incorporation of antifreeze components has a beneficial effect on the hydration heat process inside the cement paste. Figure 2 shows the heat of hydration of the sample doped with 1.5%  $\text{CaCl}_2$ , 1.0%  $\text{K}_2\text{CO}_3$ , 1.0%  $\text{NaNO}_2$  and 1.5%  $\text{Na}_2\text{SO}_4$ . The accelerated heat of hydration of the admixture is shown in Figure 2a. Compared with the reference OPC, the peak heat flow moves forward, and the acceleration effect is in the following order:  $\text{CaCl}_2 > \text{K}_2\text{CO}_3 > \text{Na}_2\text{SO}_4 > \text{NaNO}_2$ . It can be seen that the chemical admixtures accelerate the hydration reaction, and  $\text{CaCl}_2$  and  $\text{K}_2\text{CO}_3$  promote the nucleation rate of the hydration products [65].  $\text{Na}_2\text{SO}_4$  increases strength at an early stage by forming sulfoaluminate products such as Aft or AFm.  $\text{NaNO}_2$  is mainly used to maintain sufficient hydration liquid in a cement paste system at a negative temperature, providing condensed nuclei during hydration. The accumulated heat of the chemical reaction is related to the degree of hydration of the cement–water system, as shown in Figure 2b. According to the exothermic value, it can be seen that the order of increasing the heat of hydration from high to low is as follows:  $\text{CaCl}_2 > \text{Na}_2\text{SO}_4 > \text{K}_2\text{CO}_3 > \text{NaNO}_2$  [20]. Figure 3 shows the XRD analysis comparison of  $-5^{\circ}\text{C}$



mixed with 8% calcium nitrate + 1.5% sodium thiocyanate, which shows that the addition of binary antifreeze causes the hydrate phase to react and enhances the precipitation of cement hydrate [62].

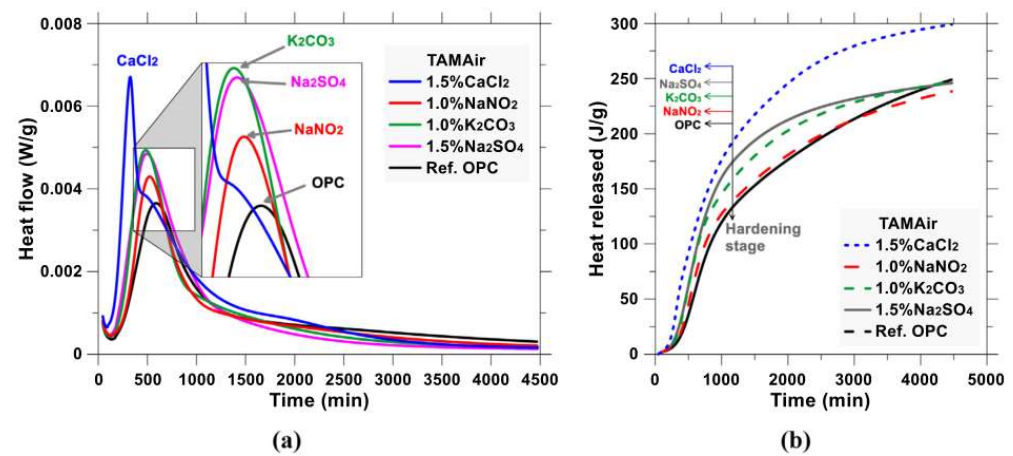


**Figure 2.** Heat of cement hydration at 1.5% CaCl<sub>2</sub>, 1.0% K<sub>2</sub>CO<sub>3</sub>, 1.0% NaNO<sub>2</sub>, 1.5% Na<sub>2</sub>SO<sub>4</sub>: (a) normalized flow, (b) accumulated heat release [20].

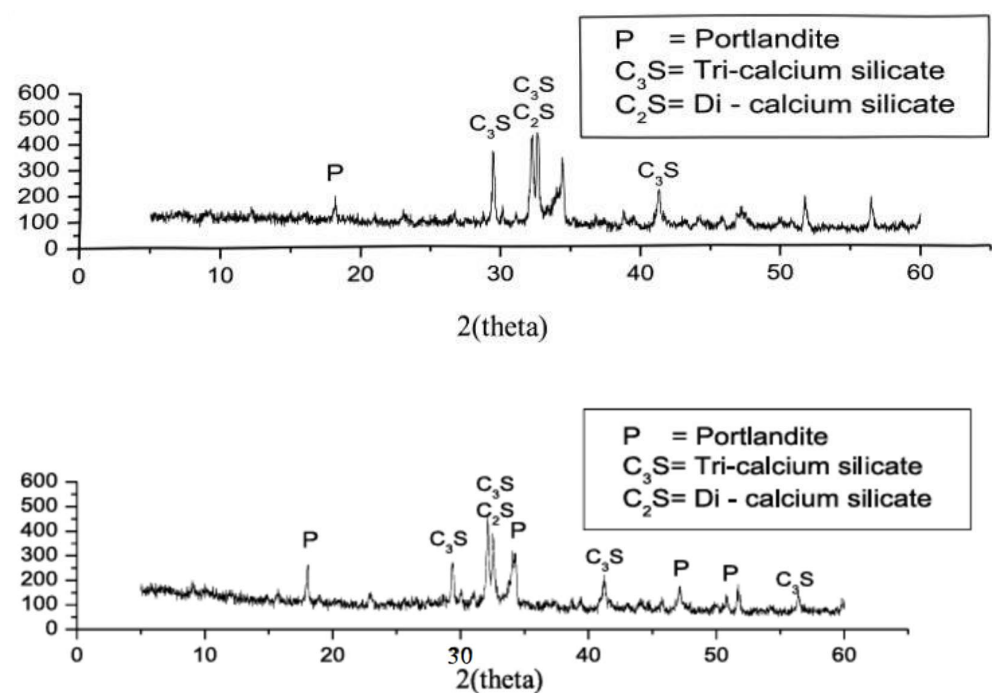


**Figure 3.** XRD analysis at  $-5^{\circ}\text{C}$  mixed with undoped 8% calcium nitrate + 1.5% sodium thiocyanate [62].

The incorporation of antifreeze components buys time for early hydration, but the incorporation of some inorganic salts does not have a completely beneficial effect on the porosity of the material. Figure 4 shows the effect of different antifreeze components on porosity under  $-1 + 1$  day curing. It can be seen that the incorporation of the four antifreeze components increases the porosity of harmful pores under the dosage. It can be seen that the incorporation of antifreeze components will not have a positive impact. It is necessary to select the appropriate antifreeze component type and dosage according to the material properties and negative temperature, or it will have a negative effect.

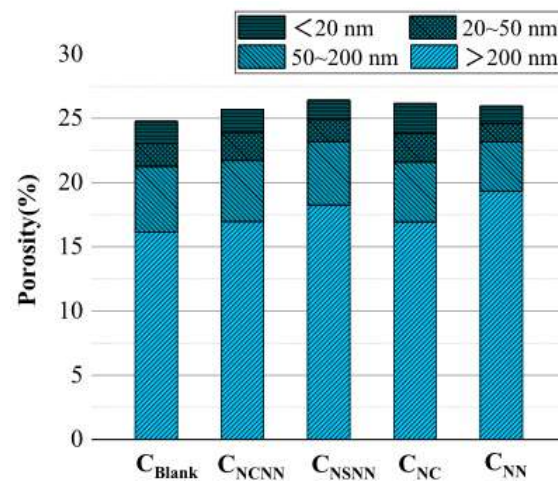


**Figure 4.** Effect of antifreeze components on pore structure under  $-1 + 1$  d curing 2% NaCl + 3% NaNO<sub>2</sub>, 2% Na<sub>2</sub>SO<sub>4</sub> + 3% NaNO<sub>2</sub>, 5% NaCl, 5% NaNO<sub>2</sub> [59].

## 2.2. Sulfate Aluminum Cement

Sulfate aluminum cement (SAC) was developed around the 1970s [33]. It is obtained by calcining bauxite, limestone, and gypsum to obtain clinker, which mainly contains C<sub>4</sub>A<sub>3</sub>S and C<sub>2</sub>S. SAC has attracted attention because of its superior performance [66,67]. At present, the construction of negative temperatures in winter in China is becoming more and more common, and the development of cement-based cementitious materials to meet the requirements of a negative-temperature environment is extremely urgent. The SAC cement-based materials cured at negative temperatures still use ettringite as the main source of strength. The number and shape of hydration products are changed by the negative-temperature curing temperature. The ettringite grown at  $-15$  °C was needle-like, and the ettringite grown at  $0$  °C was columnar. Negative-temperature curing will cause gypsum dihydrate to appear in the early hydration products and reduce the early strength, but the strength will increase significantly in the later stage [68,69]. SAC is a new type of low-carbon cement that can recycle aluminum-containing industrial waste while saving energy and reducing emissions. It will also be a low-cost cement with superior performance in the future [33].

### 2.2.1. Mechanical Properties

Under low-temperature curing, antifreeze components mixed with SAC mortar, the influence on its mechanical properties is not always a positive effect (Table 2). The compressive strength of cement mortar mixed with styrene–butadiene emulsion will not increase much, but an appropriate amount of styrene–butadiene emulsion can significantly improve the flexural strength and tensile bond strength [70,71]. The addition of a retarder has an adverse effect on the early strength of cement paste regardless of type and dosage [72].

**Table 2.** Effect of antifreeze or extraneous components on compressive strength of calcium sulfoaluminate cement-based material.

Material Type	Curing Temperature (°C)	Antifreeze Component	Optimum Content (%)	Age (d)	IRCS (%)	Refs.
Cement mortar	5	Li <sub>2</sub> CO <sub>3</sub>	20	28	25	[70,71]
	5	CaSO <sub>4</sub> ·2H <sub>2</sub> O	40	28	−29	[73]
	−10	Li <sub>2</sub> CO <sub>3</sub> + Ca(NO <sub>3</sub> ) <sub>2</sub>	Li <sub>2</sub> CO <sub>3</sub> (0.9) + Ca(NO <sub>3</sub> ) <sub>2</sub> (1)	−7	251	[74]

Table 2. Cont.

Material Type	Curing Temperature (°C)	Antifreeze Component	Optimum Content (%)	Age (d)	IRCS (%)	Refs.
Cement mortar	−20	$\text{Ca}(\text{NO}_3)_2 + \text{Al}_2(\text{SO}_4)_3$	$\text{Ca}(\text{NO}_3)_2(9) + \text{Al}_2(\text{SO}_4)_3(0.9)$	−28	13	[75]
	−20	+ $\text{C}_6\text{H}_{15}\text{NO}_3$ $\text{Ca}(\text{NO}_3)_2$	+ $\text{C}_6\text{H}_{15}\text{NO}_3(0.04)$ 5	−3 + 28	11	[43]

Note: The ‘−’ in the compressive strength increase rate indicates that the strength decreases; in the age, ‘−’ represents negative-temperature curing, ‘+’ represents positive temperature curing; the increase rate of compressive strength is based on the middle age of the table.

Under the condition of negative temperature, the content of lithium carbonate was proportional to the compressive strength, and the compressive strength reached the maximum value by adding 1.2% lithium carbonate in the first 7 days, but single-doped aluminum sulfate had a negative impact on the compressive strength at 1% dosage. When the content of lithium carbonate and aluminum sulfate is 1.2–1.5%, it has higher early compressive strength (2 h) and higher later compressive strength (7 d). Under the condition of curing at −10 °C, the mixture of lithium carbonate and calcium nitrate was added. With the increase in dosage, the compressive strength of mortar was increased at all ages. However, at the age of 1 d and 7 d, when the content exceeds 2.2%, the compressive strength of the mortar decreased [74]. The addition of lithium carbonate accelerated the early hydration process and improved the early strength (12 h–3 d), but the addition of lithium carbonate had no significant effect on the compressive strength at 7 d and 28 d. It is worth noting that the incorporation of 0.1% lithium carbonate at a positive temperature of 4 °C has an adverse effect on the compressive strength at 7 d and 28 d ages [76]. It can be seen from Table 2 that the incorporation of inorganic salt antifreeze components can basically improve compressive strength. Compared with Portland cement, SAC has superior negative-temperature strength and good development prospects in winter construction. At 5 °C,  $\text{CaSO}_4 \cdot 2\text{H}_2\text{O}$  slows down early hydration due to its slow dissolution, and the compressive strength is positively correlated with AH3 and unrelated to AFt. When 40% is added, the AH3 does not increase, resulting in a decrease in the compressive strength at 28 days [73].

### 2.2.2. Microscopic Mechanism

Low-temperature curing (0 °C and 5 °C) delayed the hydration of sulphoaluminate cement compared with 20 °C standard curing [77]. The early hydration degree was greatly reduced, and the scanning electron microscope photos of sulfate cement at 0 °C, 5 °C, and 20 °C for 1 d are shown in Figure 5. After 1 day of hydration, the formation of AFt, AFm, and AH<sub>3</sub> decreased significantly with the decrease in curing temperature. After 28 days of hydration, the amount of AFt produced at each curing temperature was basically the same, but the amount of AFm and AH<sub>3</sub> gel decreased in turn according to the curing temperature. The lower curing temperature delays the transformation of AFt to AFm in calcium sulphoaluminate cement paste [69]. The addition of calcium chloride solution with a concentration of 16–28% can prevent the freezing of fast-hardening sulfuraluminate cement slurry. When the concentration of the solution is 16%, the hydration product is mainly ettringite, which exists in the form of needle-shaped crystals. When the concentration of the solution is 22%, the hydration product is formed by Friedel’s salt, which exists as a hexagonal tabular. When the solubility of the solution is 28%, the hydration product is mainly Friedel’s salt, which exists as petal-shaped hexagonal plate-like crystals [78]. However, it is still necessary to add a retarder, as it sets too fast; all kinds of retarders will reduce the compressive strength, the best retarding effect is borax with a 0.6% dosage. Borax can inhibit the formation of ettringite in cement paste. The retarding



effect of sodium gluconate and L (+)-tartaric acid is not obvious, and the morphology and distribution of ettringite are changed, and the strength is significantly reduced [72].

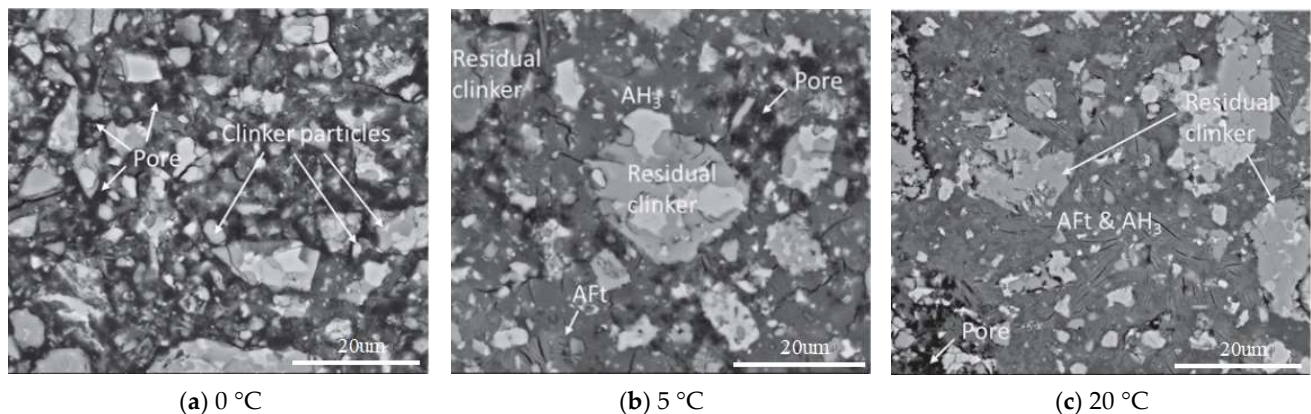


**Figure 5.** Scanning electron micrographs of SAC maintained at 0 °C, 5 °C, and 20 °C for 1 day [77].

The TG-DTG curve of cement mortar mixed with 0.6% lithium carbonate (LC) and 0.6% aluminum sulfate (AS) mixture cured at 0 °C for 7 days is shown in Figure 6. It can be seen that the mass loss of SAC with LC-AS at 40–100 °C is higher than that of SAC without LC-AS, and its improvement effect on compressive strength can be attributed to the increase of Aft production [74]. The hydration and microstructure development of cement mortar was promoted by adding 9% calcium nitrate, 0.9% aluminum sulfate, and 0.04% triethanolamine at −20 °C. Liu et al. shows that the incorporation of aluminum sulfate and triethanolamine increases the hydration products of the mortar, and the ettringite crystals are more complete and the crystal volume is larger, which improves the strength of the mortar. However, the compound hydration products of organic antifreeze urea and calcium nitrate are less, which delays the hydration and microstructure development and reduces the strength. However, the compound hydration products of organic antifreeze urea and calcium nitrate are less, which delayed the hydration and microstructure development and reduced the strength [75].

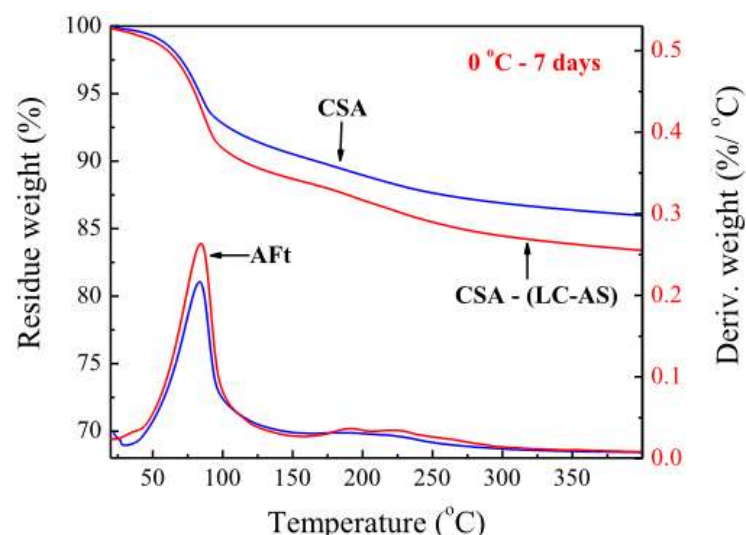


**Figure 6.** TG-DTG curves of cement mortar with and without LC-AS mixing [74].

### 2.3. Magnesium Phosphate Cement

Magnesium phosphate cement (MPC) is prepared from acid phosphate, dead-burned magnesia powder, and admixtures. Compared with Portland cement, MPC has excellent

properties such as fast-setting early strength, high bond strength, and good durability, including chemical attack resistance, ice and scaling resistance, and permeation resistance, as well as solidification and hardening at temperatures as low as  $-20\text{ }^{\circ}\text{C}$  [79,80]. Under the condition of negative-temperature curing, the magnesium phosphate cement-based material undergoes crystallization damage, and the internal capillary pore precipitates are mainly  $\text{MgKPO}_4 \cdot 6\text{H}_2\text{O}$ . The free water in the capillary cavity freezes and swells slightly, and  $\text{MgKPO}_4 \cdot 6\text{H}_2\text{O}$  crystals grow and precipitate out of the surface at the pores and microcracks inside the cement slurry, which leads to the deterioration of MPC strength under negative-temperature conditions [81]. The addition of antifreeze components will greatly improve the early mechanical properties of magnesium phosphate cement-based materials under negative-temperature curing (Table 3). The magnesium phosphate cement slurry with the content of 12% light-burned magnesium oxide was cured at a negative temperature for 2 h, and the compressive strength was increased by 450% [82,83].

**Table 3.** Effect of extraneous components on compressive strength of magnesium phosphate cement-based materials.

Material Type	Curing Temperature ( $^{\circ}\text{C}$ )	Antifreeze Component	Optimum Content (%)	Age (d)	IRCS (%)	Refs.
Concrete	$-20$	Light calcined magnesia	10	$-1\text{ d}$	198	[79]
	$-20$	Magnesia whiskers	3	$-1\text{ d}$	203	[80]
Cement paste	$-20$	Light calcined magnesia	8	$-1\text{ d}$	33	[84]
	$-10$	Light calcined magnesia	12	$-2\text{ h}$	450	[82,83]

Note: ‘ $-$ ’ represents negative-temperature curing; the increase rate of compressive strength is based on the middle age of the table.

The rapid hydration of magnesium oxide whiskers in the magnesium phosphate cement slurry released heat, which made the acid-base reaction of the MPC slurry continue at a negative temperature; the coagulation hardening speed was significantly accelerated, and the reaction temperature was also increased. At the same time, struvite is used as a crystal seed, which plays a role in inducing internal crystallization so that the MPC slurry still maintains high early strength even in severe cold environments [80]. The appropriate amount of lightly burned magnesium oxide (LBM) increased the reaction rate of MPC slurry. When the peak temperature of the exothermic reaction of MPC reaches  $60\text{ }^{\circ}\text{C}$ – $70\text{ }^{\circ}\text{C}$ , the LBM/M (reburned magnesium oxide) ratio is the optimal value, namely when the ambient temperature is  $-2\text{ }^{\circ}\text{C}$ ,  $-10\text{ }^{\circ}\text{C}$ , and  $-20\text{ }^{\circ}\text{C}$ , the appropriate proportions of LBM/M are 2–4%, 4–6%, and 8–12%, respectively.

The antifreeze component lowers the freezing point of the solution, allowing it to undergo hydration reactions at lower temperatures under negative-temperature curing, increasing its strength. When the concentrations of ethylene glycol, potassium acetate, potassium chloride, and dilute acid phosphate solution were 40%, 40%, 25%, and 20%, respectively, the freezing point of the mixed water dropped to  $-20\text{ }^{\circ}\text{C}$  (Figure 7). The compressive strength of MPC with soluble substances as an early strength agent was still improved after returning to room temperature. In the severe cold environment, the heat released by the rapid reaction of LBM and diluted PA stimulated the initial response of MPC. When the LBM/M ratio is 4–6% and 6–8%, the compressive strength of MPC can reach 30 MPa and 40 MPa at 2 h and 24 h, respectively [79].

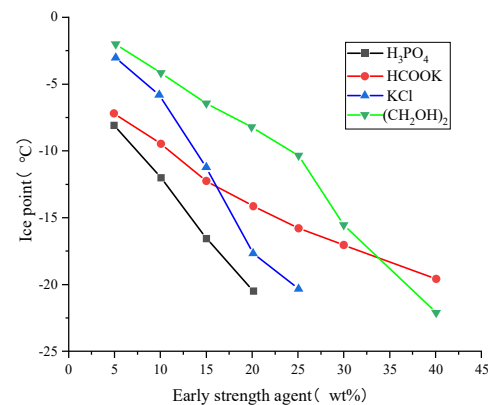


**Figure 7.** The freezing point of the solution containing the antifreeze components [79].

In the preparation process of magnesium phosphate cement, due to the double hydrolysis of monoammonium phosphate and borax, the freezing point of mixed water can be reduced to  $-10\text{ }^{\circ}\text{C}$ . In the negative-temperature environment, the fluidity and coagulation time of MPC decreased with the increase of M/P (phosphate), and the compressive strength was increased with the increase of M/P and decreased with the increase of B/M. Even if the atmospheric temperature is close to  $-20\text{ }^{\circ}\text{C}$ , the hydration rate is still dominant. The frost action does not work [84,85]. Considering the winter construction environment, the ice-breaking water is used as mixing water. The reaction heat and friction heat are released during the preparation of MPC, which melt the ice particles. The strength of magnesium phosphate cement slurry can still reach more than 25 MPa under the condition of negative temperature ( $-20\text{ }^{\circ}\text{C}$ ) curing for 3 days after ice particle mixing, and the strength of magnesium phosphate cement slurry can still reach more than 25 MPa after 1 day of curing at  $-20\text{ }^{\circ}\text{C}$ . It can be seen that the preparation and maintenance of magnesium phosphate cement slurry in a severe cold environment will not affect the strength development of magnesium phosphate cement slurry after a positive temperature [82]. The construction prospect of magnesium phosphate cement in winter is broad, but due to the high cost of raw materials, the later low-temperature research should reduce the production cost and consider the performance improvement under the small amount of admixture in order to achieve dual cost control.

#### 2.4. Alkali-Activated Cementitious Material

Geopolymer is an environmentally friendly green building material with many advantages, such as early strength, good mechanical properties, good interfacial bonding ability, good corrosion resistance, and low permeability [86,87]. It is expected to become a new type of building material that can replace Portland cement. It has been widely used in construction, transportation, marine engineering, mining engineering, and other fields [88–91]. The incorporation of admixtures into alkali-activated cementitious materials is shown in Table 4. At  $-20\text{ }^{\circ}\text{C}$ , with a 2% dosage of  $\text{NaNO}_3$ , the improvement ratio of compressive strength is 15%. Under extremely low-temperature conditions, the effect of  $\text{NaNO}_3$  is limited but provides some improvement in early strength [92]. At  $-10\text{ }^{\circ}\text{C}$  and  $5\text{ }^{\circ}\text{C}$ , with 3% and 5% dosages of  $\text{CaO}$ , the improvement ratios of compressive strength are 5% and 26%, respectively.  $\text{CaO}$  shows more significant effects at relatively higher low temperatures ( $5\text{ }^{\circ}\text{C}$ ), making it suitable for low-temperature environments [93,94]. At  $10\text{ }^{\circ}\text{C}$ , with a 0.06% dosage of  $\text{C}_6\text{H}_{15}\text{NO}_3$ , the improvement ratio of compressive strength reaches as high as 75%, indicating its remarkable enhancement performance in low-temperature environments [95] (Table 5).

**Table 4.** Effect of antifreeze components on compressive strength of alkali-activated cementitious materials.

Precursor	Activator	Curing Temperature (°C)	Antifreeze Component	Optimum Content (%)	Age (d)	IRCS (%)	Ref.
Slag	NaOH	−20	NaNO <sub>3</sub>	2	−7 + 28	15	[92]
Slag	K <sub>2</sub> SiO <sub>3</sub> and KOH	−10	CaO	3	−28	5	[93]
Slag							
Portland cement	Na <sub>2</sub> SiO <sub>3</sub>	5	CaO	5	28	26	[94]
Calcium sulfate	and NaOH						
aluminum sulfate							
cement							
Slag	Na <sub>2</sub> SiO <sub>3</sub>	10	C <sub>6</sub> H <sub>15</sub> NO <sub>3</sub>	0.06	7	75	[95]
Silica fume	and NaOH						

Note: ‘−’ represents negative-temperature curing, ‘+’ represents positive-temperature curing; the increase rate of compressive strength is based on the middle age of the table.

**Table 5.** Prices of various antifreeze components.

Antifreeze Component	Price (CNY/kg)
CaCl <sub>2</sub>	1–1.5
C <sub>2</sub> H <sub>6</sub> O <sub>2</sub>	6–8
NaNO <sub>2</sub>	4–6
Ca(NO <sub>3</sub> ) <sub>2</sub>	2–3
CO(NH <sub>2</sub> ) <sub>2</sub>	2–3
K <sub>2</sub> CO <sub>3</sub>	7–9
CNNaS	15–20
C <sub>6</sub> H <sub>15</sub> NO <sub>3</sub>	10–15
Li <sub>2</sub> CO <sub>3</sub>	200–250
CaSO <sub>4</sub> ·2H <sub>2</sub> O	0.3–0.5
Al <sub>2</sub> (SO <sub>4</sub> ) <sub>3</sub>	1.5–2.5
CaO	0.5–0.8
NaNO <sub>3</sub>	3–8

#### 2.4.1. Mechanical Properties

Consistent with OPC, the curing temperature below zero degrees delays the hydration process of alkali-activated materials, resulting in prolonged setting time [8]. Compared with OPC, the mechanical properties of alkali-activated slag (AAS) cementitious materials show an absolute advantage under low-temperature curing conditions, especially below zero temperature. However, with the decrease in curing temperature, the mechanical properties of both materials decrease to varying degrees [9,96]. Under a low temperature of 5 °C curing, all kinds of calcium-rich precursors can improve the early strength of AAS. The compressive strength of 15% Portland cement clinker is the highest in both early and late stages, whose compressive strength was increased by about 35%, followed by 12% thioaluminate cement clinker and 5% calcium oxide [94]. In the AAS slurry cured at −10 °C, the incorporation of calcium oxide increased the heat release rate and accumulated heat, which provided a feasible way to accelerate the hydration reaction of AAS below zero, and the compressive strength and flexural strength of the alkali-activated slag slurry cured were increased at −10 °C by 40% and 48%, respectively, at 1 day [93]. Under the condition of −20 °C curing, the alkali-activated mortar material is mixed with NaNO<sub>3</sub>, NaNO<sub>2</sub>, and NaCl. These three kinds of inorganic salts have improved the early strength of alkali slag cement to varying degrees. At −7 + 28 days of age, the incorporation of 2% NaNO<sub>3</sub> increased compressive strength by 14% [92].

#### 2.4.2. Microscopic Mechanism

The hydration process of alkali-activated cementitious materials can generally be divided into four stages: the ion dissolution and release stage, ion reconstitution stage, the hardening acceleration stage, and the hardening deceleration stage. The resistivity method was used to dynamically reflect the early hydration process of alkali-activated cementitious materials, and the resistivity method results showed that the negative-temperature curing extended the duration of each stage and delayed the start of the next stage [97]. The freezing point of water in the liquid phase system of alkali slag was decreased, and the existence of free water is maintained by the doping of  $\text{NaNO}_3$ ,  $\text{NaNO}_2$ , and  $\text{NaCl}$ . The hydration reaction of alkali slag cement was accelerated, and the early strength of alkali slag cement under the condition of negative temperature was improved. The late compressive strength is improved to a certain extent under the condition of low dosage [92]. The incorporation of  $\text{CaO}$  made the structure more denser (Figure 8), accelerated the slag hydration reaction, and increased the generation of  $\text{Ca}(\text{OH})_2$ . The addition of  $\text{CaO}$  at the same time can improve the early heat release rate and cumulative heat. It is beneficial to accelerate the release of  $\text{Si}(\text{OH})_4$ ,  $\text{Al}^{3+}$ , and  $\text{Ca}^{2+}$  from slag raw material particles, which promote polymerization and formation of C(-A)-S-H [93]. Under the condition of a curing temperature of 5 °C, calcium-rich precursors can increase the early strength of AAS by about 35%, reduce the early total porosity of AAS, increase the thickness of the hydration product layer, and improve the microstructure. The internal  $\text{Ca}(\text{OH})_2$  and limestone powder can play a micro-filling role and improve the early strength of AAS in low-temperature environments [94].

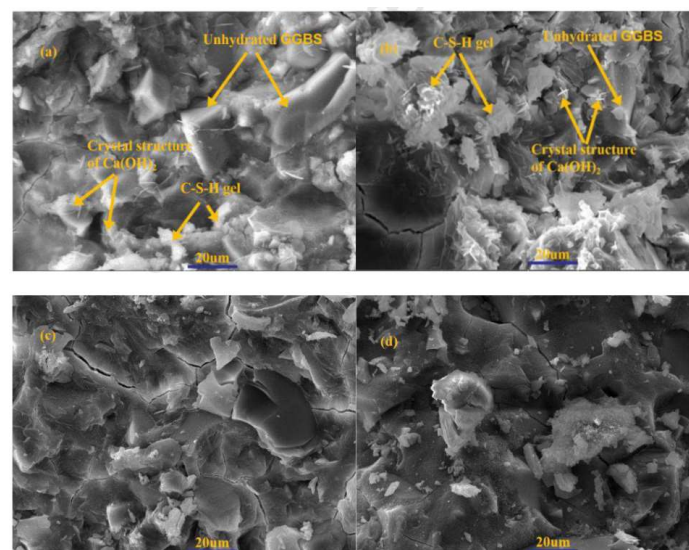


**Figure 8.** The microstructure of AAS mortar was cured at  $-10\text{ }^{\circ}\text{C}$  and  $20\text{ }^{\circ}\text{C}$  for 7 days. (a)  $-10\text{ }^{\circ}\text{C}$  AAS, (b)  $-10\text{ }^{\circ}\text{C}$  AAS + 3%  $\text{CaO}$ , (c)  $20\text{ }^{\circ}\text{C}$  AAS, (d)  $20\text{ }^{\circ}\text{C}$  AAS + 3%  $\text{CaO}$  [93].

The addition of alkali-activated materials to triethanolamine, triisopropylamine, and lithium carbonate can improve the microstructure at a negative temperature (Figure 9). After adding 0.06% triethanolamine, the geopolymer mortar hydrates more fully, and the hydrated crystal structure is denser, indicating that triethanolamine is more suitable to improve the negative-temperature mechanical properties of slag silica fume geopolymer mortar. The unsaturated N and O atoms in triethanolamine can form complexes with  $\text{Ca}^{2+}$  and  $\text{Al}^{3+}$  produced in the hydration process of geopolymer mortar, reduce the concentration of  $\text{Ca}^{2+}$  and  $\text{Al}^{3+}$ , and promote the hydration of geopolymer mortar. In addition, the complexes formed by triethanolamine and  $\text{Ca}^{2+}$  and  $\text{Al}^{3+}$  ions adhere to the surface of slag and silica fume particles, and these ions blocked the inhibition of the hydration reaction of



slag and silica fume by the hydration product C-S-H gel, accelerated the formation rate of hydration products, and then improved strength.

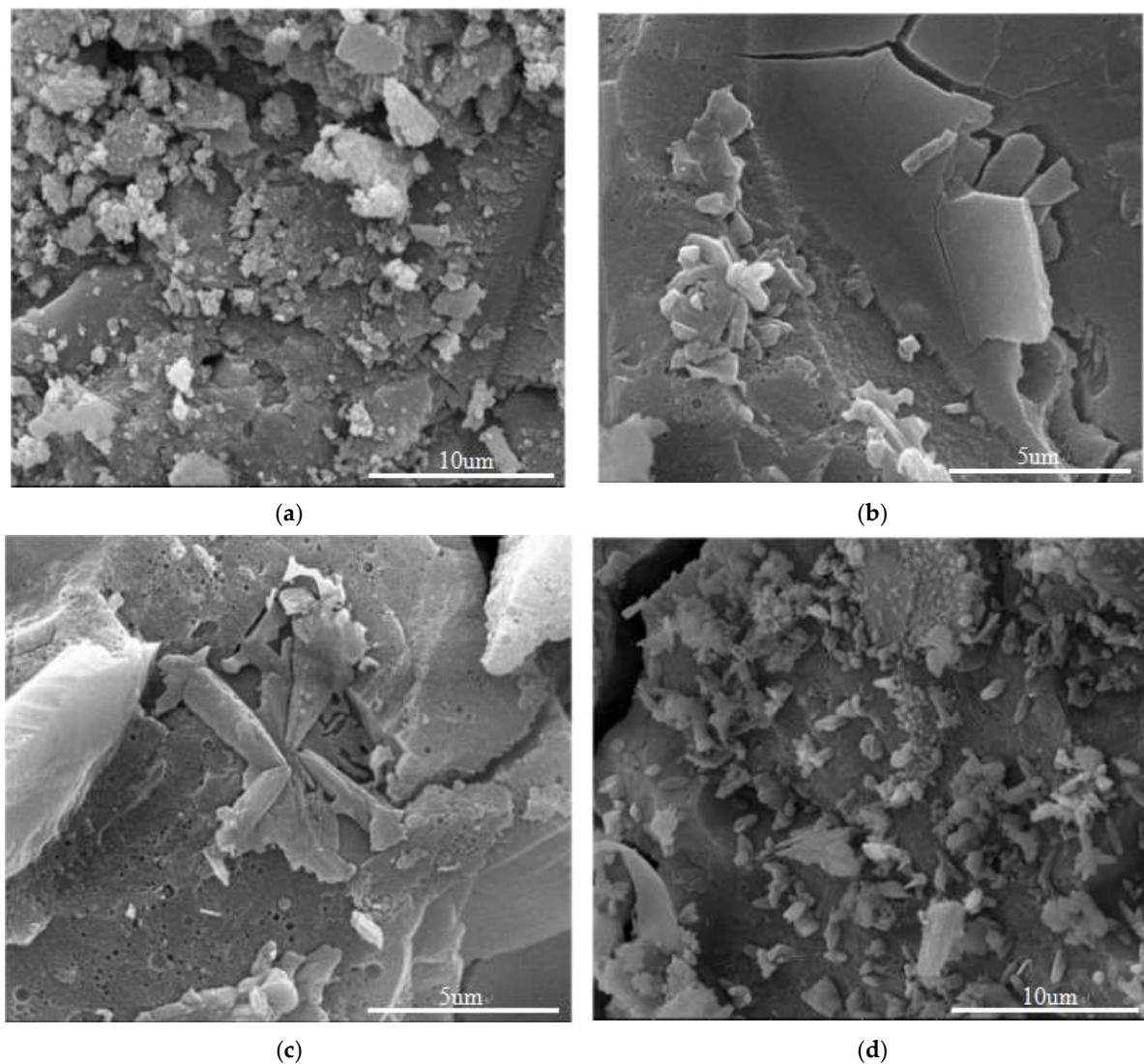


**Figure 9.** Effect of different early strength agents on the micromorphology of geopolymer mortar (a) unadulterated, (b)  $\text{Li}_2\text{CO}_3$ , (c)  $\text{C}_6\text{H}_{15}\text{NO}_3$ , (d) triisopropylamine [95].

Due to the wide variety of precursors and activators, alkali-activated cementitious materials are mostly researched for high temperature and standard curing. The research on negative temperature started late, and the incorporation of various antifreeze components was less than that of other cementitious materials. The study of low-temperature performance suggests that the precursor and activator with good low-temperature performance should be selected for configuration. Under the condition of reducing the freezing point of the solution and taking into account the mechanical properties, for different negative-temperature conditions, it is necessary to first select the appropriate antifreeze component and admixture type and content, and further combine with the pre-curing measures. Due to the characteristics of fast hardening and early strength of alkali-activated cementitious materials, the time and cost of the pre-curing system can be significantly reduced. At the same time, it is also necessary to consider whether the incorporation of some inorganic salts will have an adverse effect in the pre-curing stage and whether the role of inorganic salts can play normally under the negative-temperature conditions after the pre-curing stage.

### 3. Effects of Admixtures and Nanoparticles on the Mechanical Properties and Microstructure of Ordinary Cement-Based Materials Under Low-Temperature Curing

In the prevention measures of low-temperature frost damage of building materials under low-temperature curing conditions in winter, in addition to the incorporation of various inorganic salt antifreeze agents to reduce the freezing point of the hydration slurry solution and prolong the hydration time, the incorporation of various beneficial materials increases the compactness of the hydration slurry, accelerates the early hydration reaction, and can also reduce the low-temperature frost damage. The effects of admixtures on the properties of cement-based materials under low-temperature curing were sorted out from three aspects: mineral admixtures, nanomaterials, and hydrated calcium silicate seeds [97–99].

#### 3.1. Mineral Admixtures

A large amount of industrial waste is produced in industrial production. These industrial solid wastes contain a large amount of non-renewable mineral resources, which are discharged at will to damage the environment. Therefore, scholars at home and abroad turn these industrial solid wastes such as slag, fly ash, and silica fume into treasure and add them to building materials such as concrete as mineral admixtures [100–102].

##### 3.1.1. Mechanical Properties

The mechanical properties of cement-based materials under low-temperature curing can be improved by single and compound addition of fly ash and silica fume. The influence of silica fume is greater. When the optimal dosage is 6%, compared with the control group, the compressive strength of the cement-based materials increases by 37% under  $-10\text{ }^{\circ}\text{C}$  curing and  $-7 + 56$  days (Table 6). However, with the decrease in curing temperature, the compressive strength growth became smaller. Therefore, it can be seen that mineral admixtures have a limited effect on the mechanical properties of cement-based materials at low temperatures.

**Table 6.** Effect of mineral admixtures on compressive strength.

Material Type	Curing Temperature ( $^{\circ}\text{C}$ )	Admixture Type	Optimum Content (%)	Age (d)	IRCS (%)	Ref.
Concrete	−5	Fly ash + Silica fume	10 + 5	−7 + 28	19	[21]
	−10	Silica fume	6	−7 + 56	37	[22]
	−20	Silica fume	7	−7 + 56	12	[103]
Cement paste	Winter natural conservation	Fly ash	25	572	21	[104]
	−5	Silica fume	8	−14	15	[105]

Note: ‘−’ represents negative-temperature curing, ‘+’ represents positive temperature curing; the increase rate of compressive strength is based on the middle age of the table.

##### 3.1.2. Microscopic Mechanism

Silica fume improved the density of the cementitious system, but the lower curing temperature inhibited the volcanic ash activity of silica fume. A large amount of  $\text{SiO}_2$  in silica fume can undergo a secondary hydration reaction with the cement hydration product  $\text{Ca}(\text{OH})_2$ , which increases the number of hydration products of the cementitious material and is also conducive to the improvement of the strength of the composite cementitious system. With the progress of the hydration process, the product precipitated to a certain extent, and the secondary reaction of silica fume entered the acceleration period, which

provided the possibility for the improvement of the strength in the later stage of curing. Comparing the calcium hydroxide content in the slurry containing and not containing silica fume, it was found that the activity of water decreased with the temperature decreased, and the hydration was inhibited, resulting in a decrease in calcium hydroxide content. With the increase in temperature, the content of  $\text{Ca}(\text{OH})_2$  in silica fume-silicate cement increased first and then decreased [106]. It can be seen from Figure 10 that the addition of silica fume reduces the porosity of the system and improves the pore size distribution of the system, especially the number of macropores [105]. Under the same conditions, the strength of concrete with 6% silica fume is the highest among all the prepared specimens, and the frost resistance and chloride ion penetration resistance of negative-temperature concrete are the best [22].

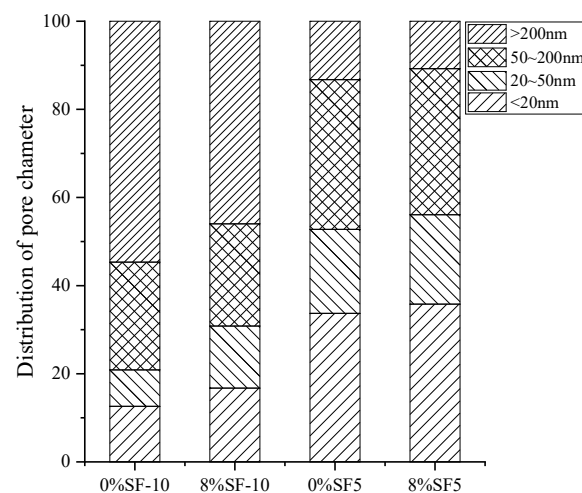


**Figure 10.** Pore size distribution of the sample at 7 days [105].

The micro-aggregate filling effect and secondary hydration reaction of the mineral admixture further improved the microstructure of the interface transition zone of the negative-temperature concrete. The appropriate amount of mineral admixture was helpful in forming a good interface microstructure of mortar and concrete undergoing negative-temperature action. The early hydration of the incorporation of fly ash was slow, but the pore structure of fly ash was refined, which made the pore size distribution more uniform, the compactness was improved, and the frost heave pressure was reduced, so that the later strength continued to develop. The rapid hydration of silica fume improved the early strength, so the double-doped fly ash and silica fume complemented each other, which can more effectively exert the micro-aggregate effect and secondary hydration effect of the two to make the structure denser [21]. However, the optimum dosage of the two materials for different materials needs further study.

### 3.2. Nanomaterials

Nanomaterials have been used in experimental research to improve the mechanical properties of low-temperature materials because of large specific surface area and good dispersibility, refinement of hydration slurry pores, and increase of compactness. Nano  $\text{CaCO}_3$  is white powder. Nano  $\text{SiO}_2$  is an amorphous white loose powder. The microstructure of these two nanomaterials is spherical, and the microscopic morphology is shown in Figure 11 [107,108].

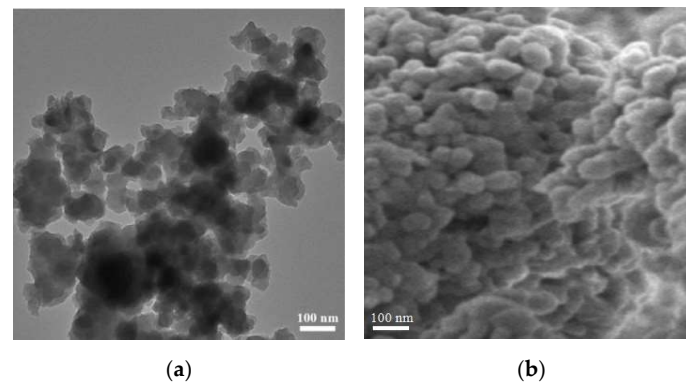


**Figure 11.** Scanning electron microscope photographs of (a)  $\text{SiO}_2$  [107], (b)  $\text{CaCO}_3$  [108].

### 3.2.1. Mechanical Properties

Nanomaterials can improve the mechanical properties of cement-based materials at low temperatures. The incorporation of Nano  $\text{TiO}_2$  can significantly improve the early mechanical properties of cement mortar under low temperature ( $5^\circ\text{C}$ ) curing, and the optimal content of 1% can be increased by more than 1 times (Table 7). The reaction mechanism is mainly that the addition of  $\text{TiO}_2$  shortened the solidification time and increased the rate of hydration heat. Nano- $\text{TiO}_2$  refined the microstructure and made it denser due to the small size effect and filling effect. By adding  $\text{TiO}_2$ , the growth of  $\text{Ca}(\text{OH})_2$  crystals was slowed down, and the size of  $\text{Ca}(\text{OH})_2$  was reduced [109]. In terms of low-temperature curing temperature of  $5^\circ\text{C}$ , the strength of the mortar increased with the increase of Nano- $\text{TiO}_2$  content from 0.25% to 1%. Compared with high temperature and standard curing, the relative compressive strength increase ratio was the largest at low temperature, namely the lower the curing temperature, the greater the positive effect of  $\text{TiO}_2$  addition on compressive strength.

**Table 7.** Effect of nanomaterial incorporation on compressive strength.

Material Type	Curing Temperature ( $^\circ\text{C}$ )	Nanomaterial	Optimum Content (%)	Age (d)	IRCS (%)	Ref.
Concrete	6.5	$\text{CaCO}_3$	2	28	2	[110]
	−5	$\text{SiO}_2$	1.2	−120	5	[107]
Cement mortar	−15	$\text{SiO}_2$	0.9	−7 + 28	23	[98]
	5	$\text{TiO}_2$	1	7	114	[109]
	5	$\text{SiO}_2$	3	28	10	[111]

Note: ‘−’ represents negative-temperature curing; ‘+’ represents positive temperature curing; the increase rate of compressive strength is based on the middle age of the table.

### 3.2.2. Microscopic Mechanism

Nano- $\text{SiO}_2$  particles can react with calcium hydroxide to form additional C-S-H gel, which is called a volcanic ash reaction. Early freezing damage affects the structure of C-S-H gel formation and reduces the degree of hydration and the content of C-S-H gel to a certain extent. The mass of  $\text{Ca}(\text{OH})_2$  consumed by Nano- $\text{SiO}_2$  in the negative-temperature frozen samples (1.17%) was lower than that in the non-frozen samples (4.89%), indicating that the early frost damage weakened the activity of Nano-silica in the cement system. Early frost damage can change some small pores (20~100 nm) into large pores (100~300 nm). Nano- $\text{SiO}_2$  particles can reduce the pores between 100 nm and 300 nm by additional formation of C-S-H gel and physical particle filling. Compared with the control group, the volume change rate of pores (100–300 nm) of the samples with Nano- $\text{SiO}_2$  (19%) was significantly lower than that of the samples without nano- $\text{SiO}_2$  (63%), indicating that nano- $\text{SiO}_2$  particles



repaired some of the degraded pores (mainly 100–300 nm) and compensated for the loss of hydration caused by early freezing damage [98].

As can be seen from Figure 12, compared with the pure cement slurry, the volume of gel pores and macroscopic pores of Nano-SiO<sub>2</sub> modified cement slurry decreased (yellow label), and the capillary pore volume increased (red label). Nano-SiO<sub>2</sub> can reduce the gel pore volume and macroscopic pore volume, and at the same time increase the capillary pore volume and refine the pore structure. Nano-SiO<sub>2</sub> mainly hindered the diffusion of chloride ions by increasing the tortuosity and decreasing the threshold diameter, thereby improving the long-term impermeability of negative-temperature cement slurry. Under the three water-cement ratios, the threshold particle size of the Nano-SiO<sub>2</sub> modified cement slurry was lower than that of the pure cement slurry, indicating that the incorporation of Nano-SiO<sub>2</sub> reduced the pore connectivity of the cement matrix. In addition, with the increase of the water-cement ratio, the improvement effect of Nano-SiO<sub>2</sub> on the threshold particle size of concrete is also more obvious [107]. Nano-SiO<sub>2</sub> significantly increased the curvature of the pore structure, which in turn increased the difficulty of chloride ion transport in the cement matrix. In the case of a low water-cement ratio, Nano-SiO<sub>2</sub> increased the tortuosity of the pore structure. In the case of a high water-cement ratio, Nano-SiO<sub>2</sub> mainly reduced the connectivity of the pore structure, and the refinement effect of Nano-SiO<sub>2</sub> on pore structure made the chloride ion transport channel more complex and chloride ion transport more difficult, thereby improving the impermeability of cement slurry.

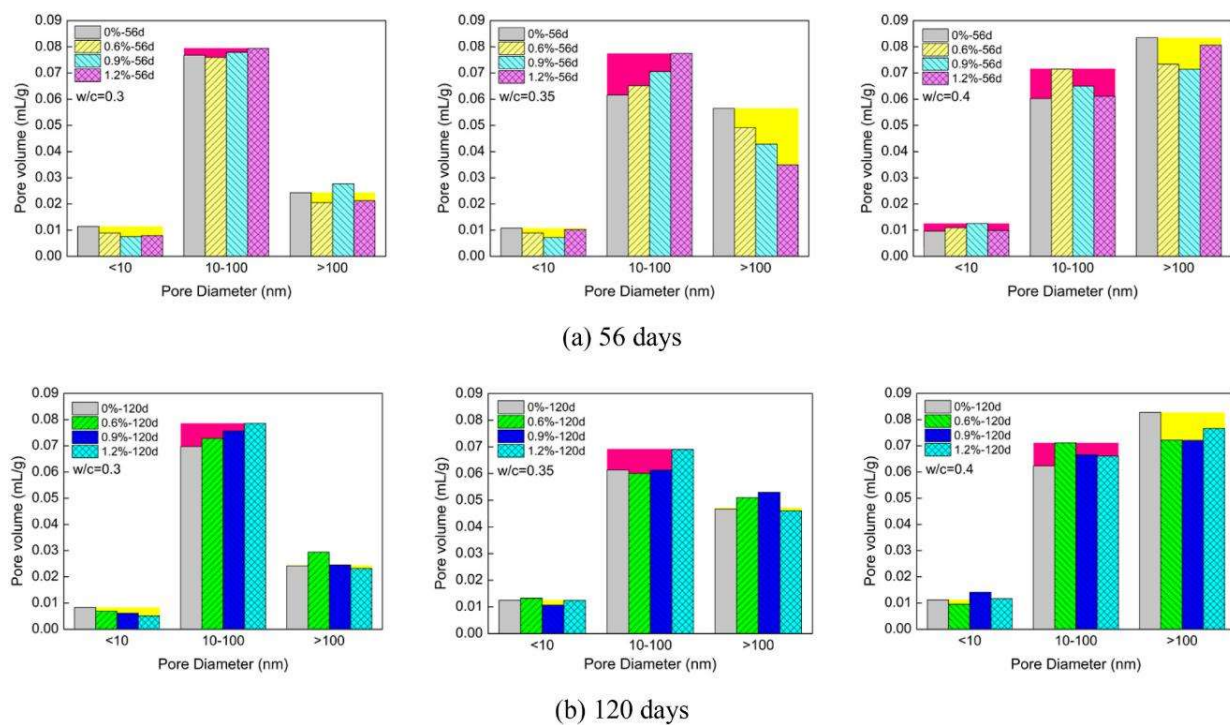


**Figure 12.** Pore volume distribution of Nano-SiO<sub>2</sub> modified cement slurry with different water-cement ratios [107].

### 3.3. Hydrated Calcium Silicate

Calcium silicate hydrate (C-S-H) seed crystal, as a new type of mineral accelerator, has attracted wide attention due to its high efficiency and chlorine-free [112,113]. The hydrated calcium silicate solution is a white liquid, and the microscopic morphology is shown in Figure 13.



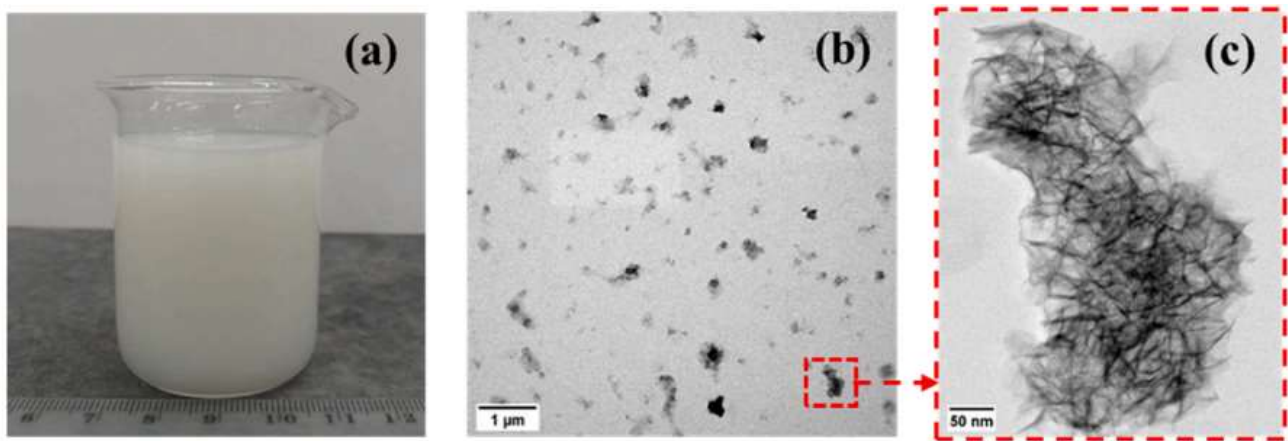


**Figure 13.** (a) C-S-H solution (b,c) TEM image of agglomeration during preparation and magnification [99].

### 3.3.1. Mechanical Properties

The strength of cement paste cured at  $-5^{\circ}\text{C}$  is much lower than that cured at room temperature for 28 days due to the serious frost damage at negative temperature. The addition of C-S-H significantly increased compressive strength (Table 8), and the compressive strength increased with the increase of C-S-H dosage. When the dosage of C-S-H was 5 wt%, the strength of 28 d can reach 34.3 MPa at negative temperature. When the pre-curing time at negative temperature is 4 h, it basically reaches the strength of cement slurry cured at room temperature for 28 days [114]. When curing at  $-10^{\circ}\text{C}$  for 28 d, the compressive strength of cement paste with 6% C-S-H content can be increased by 13%. This is because the increase of C-S-H helps to fill the pores, thereby reducing the number and size of capillary pores, improving the compactness and durability of the material, and thus increasing the compressive strength [99].

**Table 8.** Effect of hydrated calcium silicate incorporation on compressive strength.

Material Type	Adding Mode	Curing Temperature ( $^{\circ}\text{C}$ )	Optimum Content (%)	Age (d)	Control Group (MPa)	Experimental Group (MPa)	IRCS (%)	Ref.
Cement paste	Liquid reagent with C-S-H seed solid content of about 23.7%	$-10$	6	$-28$	-	15	13	[99]
	Liquid reagent with C-S-H seed solid content of 24.46%	$-5$	5	$-28$	12.21	34.3	181	[114]
Concrete	Hydrated calcium silicate suspension	$-5$	1	$-7$	9.4	15.5	65	[115]

Note: ‘ $-$ ’ represents negative-temperature curing; the increase rate of compressive strength is based on the middle age of the table.

### 3.3.2. Microscopic Mechanism

With the increase of C-S-H crystal content, the slurry microstructure became denser (Figure 14). The addition of C-S-H seeds amplified the beneficial effects of pre-curing, thereby increasing the hydration of the seed slurry, which can be attributed to the nucleation and acceleration effects of the seed embedded in the slurry and the lower amount of frozen water. C-S-H seed was beneficial for the formation of  $\text{Ca}(\text{OH})_2$  after curing on the first day, and the presence of seed can reduce the apparent energy of the precipitation process of C-S-H gel, thereby promoting the precipitation-growth process of the gel. The presence

of C-S-H seeds in the solution further promoted the precipitation of C-S-H gel on calcium hydroxide [99]. Under the curing condition of  $-5\text{ }^{\circ}\text{C}$  to  $5\text{ }^{\circ}\text{C}$ , a 2% hydrated calcium silicate solution can promote the formation of denser ITZ of mortar under negative-temperature curing conditions [116].

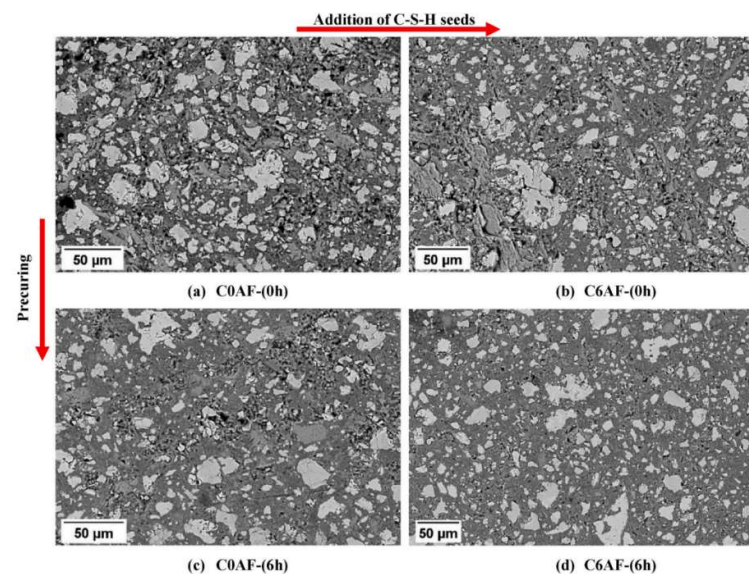


**Figure 14.** Effect of 6 h pre-curing and C-S-H seed on the microstructure compactness of 28 days slurry prepared with binary antifreeze [99].

## 4. Relationship Between Pre-Curing Time and Frost Resistance Critical Strength

### 4.1. Determination of Critical Strength of Frost Resistance

In order to smoothly carry out the construction work of concrete projects in winter and set a reasonable pre-curing time, the concept of frost-resistant critical strength of concrete was proposed, namely the minimum compressive strength that should be achieved before the fresh concrete is frozen. After being frozen, it is transferred to the positive temperature standard curing for 28 days, and its compressive strength can still reach 95% of the design standard. The research on the critical strength of frost resistance in China can be traced back to the 1980s. As early as the GBJ204-1983 [117], it was stipulated that the critical strength of concrete poured in winter before freezing refers to concrete without antifreeze. It is stipulated that the compressive strength of concrete poured in winter shall not be less than the following provisions before freezing: 30% of the design number of concrete prepared with Portland cement or ordinary Portland cement; Concrete prepared with slag Portland cement is 40% of the design mark.

However, the freezing temperature, mode, and age selection all seriously affected the judgment of scholars at that time on the value of the critical strength of frost resistance. Subsequently, the study of the critical strength of frost resistance of concrete mixed with antifreeze also became an urgent task at that time, but due to the different materials used in the preparation of samples in various experimental studies and whether the antifreeze or other beneficial components are added or not cause the data put forward by each research unit to vary greatly [118–122]. Such as SUN Wuer [123] studied the influence of different conditions such as concrete grade under variable temperature curing on the critical strength of frost resistance. The critical strength of frost resistance varies greatly, and at first, he believed that the critical strength of frost resistance is basically not related to the strength grade of concrete, but the follow-up scholars overturned this conclusion. The critical strength of frost resistance is greatly affected by negative temperature, freezing mode,

water–glue ratio, antifreeze content, and strength grade [27,123,124]. It is difficult to have a unified evaluation standard (Table 9). However, in the later period, most scholars believed that the curing method was negative-temperature curing within 7 days and standard curing for 28 days.

Subsequently, in 2011, the critical strength of frost resistance was refined. JGJ104-2011 [125] stipulates that: the frost resistance critical strength of ordinary concrete constructed by heat storage method, warm shed method, and heating method should be 30% of the designed concrete strength standard value, the concrete prepared with slag Portland cement should be 40% of the designed concrete strength standard value, but when the concrete strength grade is C10 and below, it should be greater than 5 MPa. Concrete mixed with antifreeze should be greater than 4 MPa when the minimum outdoor temperature is not less than  $-15^{\circ}\text{C}$  and more than 5 MPa when the minimum outdoor temperature is not less than  $-30^{\circ}\text{C}$ . For concrete with a strength grade equal to or higher than C50, it should not be less than 30% of the designed concrete strength grade value. For concrete with impermeability requirements, it should not be less than 50% of the designed concrete strength grade. For concrete with frost resistance durability requirements, it should not be less than 70% of the designed concrete strength grade.

**Table 9.** Relationship between pre-curing time and frost resistance critical strength.

Strength Grade	Curing Temperature ( $^{\circ}\text{C}$ )	Pre-Curing Time (h)	Frost Resistance Critical Strength (MPa)	Age (d)	Ref.
C30	−25	18	5	−1 + 28	[121]
C30	−10	18	3.6	One freeze + 28	[118]
C20					
C30	−19~−2	12	3.63	−7 + 28	[123]
C40					
C20	−25	16	1.5	−2 + 28	[126]
C25	Winter natural conservation −32~18	16	1.5	120	[127]
C30	−15	-	1.5	−28 + 28	[128]
C60	−15	15	16.4	−7 + 28	[129]
C30	−15	8	1.9	−7 + 28	[130]
C60	−10	28	3.5	−7 + 28	[131]
C35	−15	2	4.2	−7 + 28	[124]
C50	−10	28	3.5	−7 + 28	[132]
C35	−20	18	3.7	−3 + 25	[133]
	once freeze under air ( $-20^{\circ}\text{C}$ )	18	3.7		
C35	once freeze after soaking (soaking 4 h)	34	7.8	−3 + 25	[27]
	repeatedly freeze (Freeze–thaw 6 cycles)	32	7.0		
	0	16	5.2		
C50	−5	24	11.8	−3 + 28	[134]
	−10	29	16.2		
	−5	16	5.3		
C30	−10	20	9.5	−4 + 60	[135]
	−15	20	9.5		
	−20	24	11.2		
	−5	18	6.6		
C30	−10	24	8.1	−7 + 28	[136]
	−15	36	12.2		

Note: ‘−’ represents negative-temperature curing, ‘+’ represents positive temperature curing.

The minimum frost resistance critical strength and the corresponding pre-curing time in the research results of each reference are selected to provide a reference for the later winter construction. According to Table 9, most scholars choose the negative-temperature freezing temperature of  $-5\text{ }^{\circ}\text{C}$  to  $-20\text{ }^{\circ}\text{C}$  according to the actual winter engineering conditions in China, and the pre-curing time ranges from 2 h to 72 h. Experimental data show that the critical strength of freezing is mostly about 1.5–15 MPa. The research on the critical strength of frost resistance still needs to be accelerated by later scholars to determine the critical strength value of materials under different working conditions. Most scholars determined the critical strength of frost resistance of specimens based on the compressive strength guarantee rate under negative-temperature freezing conditions. Whether there are limitations is also the focus of follow-up research, so that the state can formulate more detailed relevant regulations.

#### 4.2. Effect of Porosity and Pre-Curing Time on the Critical Strength of Frost

When pouring concrete materials under low-temperature conditions, the hydration process is blocked or stagnated, the water freezes and expands to form an internal loose structure, the harmful pores increase and the performance deteriorates. Pre-normal temperature curing measures are taken to accelerate hydration, and the amount of frozen water in the hydrated slurry is consumed to form an early structure, reaching its frost resistance critical strength, thereby resisting the influence of late negative-temperature freezing [14–16]. In the study of early negative-temperature freezing damage of concrete, it is found that there is a good correspondence between the reduction of harmful pores, the reduction of strength loss, and the reduction of residual deformation in the specimen. From Figure 15, it can be seen that with the extension of pre-curing time, the harmless pores of the specimen increase significantly [59].

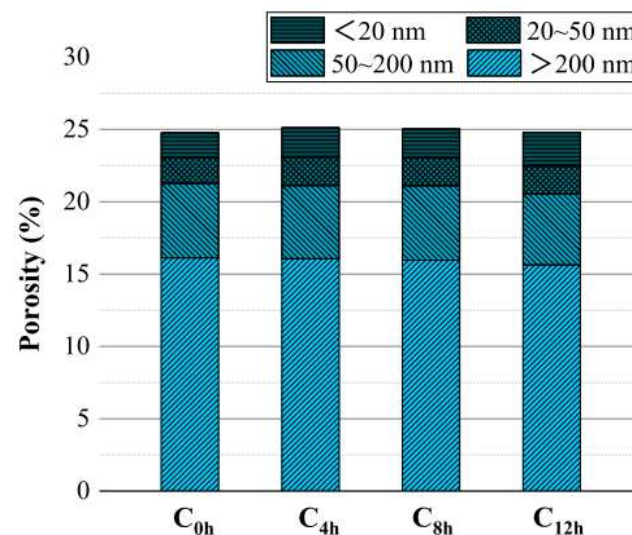


Figure 15. The effect of pre-curing time on the porosity of the specimen [59].

Zhuangzhuang Liu [20] designed three pre-curing times of 400 min, 1440 min, and 2000 min to study the influence degree of cement mortar under  $5\text{ }^{\circ}\text{C}$  curing conditions. According to the mechanical test results, it was unexpectedly found that the strength of the specimen with 400 min pre-curing time was the highest. The same trend was also observed in cement mortar containing chemical accelerators. The unexpected finding suggests that longer pre-curing at low temperatures ( $5\text{ }^{\circ}\text{C}$ ) is not always appropriate. In the case of curing temperature below zero, the longer the pre-curing time is, the more favorable it is. It

should be considered comprehensively according to the different factors such as curing system and material properties.

The determination method of frost resistance critical strength is mostly evaluated by the compressive strength guarantee rate (95%) and frost resistance durability guarantee rate (95%). After a certain pre-curing time, even if the critical strength of frost resistance is reached, the ratio of the loss rate of freeze–thaw strength and the permeability coefficient of 50 times is greater than 110%. When the frost resistance is taken as the index, the critical strength of the frost resistance of negative-temperature concrete was relatively larger than that when the compressive strength is taken as the index. The main reason is that the frost resistance index is more sensitive to the irremediable microcracks caused by the early frost damage of negative-temperature concrete, and can more truly reflect the damage of early frost damage of negative-temperature concrete to later maintenance than the compressive strength index. Based on the two indexes of compressive strength and frost resistance, the critical frost resistance strength and the corresponding pre-curing time of negative-temperature concrete under C30–C60 strength grade were studied, the higher the frost critical strength of the material with higher strength grade, the longer the pre-curing time required, the frost resistance critical strength based on frost resistance was greater than that of compressive strength, and C60 required pre-curing for up to 4 days to reach its frost critical strength. Regardless of the addition of inorganic antifreeze or organic antifreeze, the critical strength of frost resistance can be reduced, namely the pre-curing time can be reduced. The incorporation of antifreeze can effectively reduce the critical strength of frost resistance by about 5–10 MPa, and the pre-curing time can be reduced by 12–48 h [28,29]. At present, combined with engineering practice and laboratory conditions limitation, the compressive strength guarantee rate (95%) is more used to evaluate the frost resistance critical strength of materials. The relationship between the pre-curing time and the critical strength of frost resistance based on the compressive strength index and the frost resistance guarantee rate is shown in Table 10.

**Table 10.** Relationship between frost resistance critical strength and pre-curing time based on frost resistance and compressive strength guarantee rate.

Type		Frost Resistance		Compressive Strength	
		Frost Resistance Critical Strength (MPa)	Required Pre-Curing Time (h)	Frost Resistance Critical Strength (MPa)	Required Pre-Curing Time (h)
C30	Adding antifreeze	24.6	96	13.2	48
		19.6	48	5.8	18
C40	Adding antifreeze	33.6	72	17.4	36
		27.5	48	7.8	14
C50	Adding antifreeze	40.4	72	24.1	36
		31.7	36	23.6	24
C60	Adding antifreeze	49.5	96	33.2	36
		40.5	48	29.1	24

With the development of scientific research digitization and precision, the selection of an appropriate amount of antifreeze and pre-curing in winter negative-temperature construction projects complement each other, which affects the critical strength of frost resistance together. The change in pre-curing temperature will also affect the critical strength of frost resistance. Liu Zhongyang etc. [136] selected two temperatures of 30 °C



and 40 °C for electric heat tracing pre-curing and tested the material properties under a freeze-to-standard curing mode (−15 °C to −5 °C). The pre-curing time at 40 °C (18–36 h) is shorter than that at 30 °C (36–48 h). The critical frost strength of the material under 30 °C pre-curing is greater, and the strength of  $-7 + 28$  d is also better than the compressive strength of the pre-curing material under 40 °C. The range of the critical frost strength of concrete under electric heat tracing pre-curing is 6.6–17.8 MPa, which is 22.0–59.3% of the standard value of the compressive strength of concrete cubes. Su Xiaoning et al. [130] studied the concrete mixed with antifreeze. Under the condition of pre-curing for 7.48 h, it had frost resistance when the critical strength of frost resistance was zero. However, only for an example. The actual situation of the project is affected by many factors, and so is the critical strength of frost resistance. It is necessary for scholars to speed up the pace of construction research on negative-temperature live projects, and strive to form a reference system suitable for different environments, materials, and strengths as soon as possible.

#### 4.3. The Relationship Between Pre-Curing and Material Properties

Pre-curing has an important influence on the properties of concrete materials, some properties such as compressive strength, frost resistance, microstructure, and so on. It is helpful to improve the performance of concrete by appropriate pre-curing time.

The longer the pre-curing time, the better the properties of concrete. Yi [137] et al. showed that the damage degree of compressive strength of frozen concrete was significantly reduced after 6 h of pre-curing; Zhang [59] et al. found that pre-curing is one of the important factors in reducing the frost deformation of early frozen concrete.

As the pre-curing time increases, the corrosion resistance improves. Liu [138] et al. short-term freeze the specimens with a water-binder ratio of 0.4 at 24 and 72 h, respectively, and then soak them in water above 0 °C for 28 d. The study found that the shorter the pre-curing time, the more serious the early freeze–thaw damage of concrete; after freezing and thawing, the specimens were subjected to subsequent water curing, and it was found that the compressive strength recovery rate was increased to more than 60%.

As the pre-curing time increases, the internal porosity decreases, and the number and width of cracks in the interfacial transition zone between layers also decrease. Li [139] et al. found that the longer the inter-layer pouring time of RCC specimens, the shorter the pre-curing time, the greater the internal porosity, and the more and wider the thickness of the cracks of the interface transition zone between the layers. The thickness of the interfacial transition zone between the RCC layers after 24 h of pouring and pre-curing for 12 h is 5.6 µm, while the internal crack width of the unfrozen RCC specimen is only 1.2 µm.

## 5. Discussion and Outlook

Under the condition of negative temperatures in winter, the performance of building materials such as concrete will be significantly affected. Therefore, it is of great significance to study how to improve the performance of these materials in low-temperature environments. This paper reviews the effects of additives, admixtures, and pre-curing measures on the properties of cement-based materials and alkali-activated materials under low-temperature curing.

### 5.1. Effect of Additives on Material Properties

In the study of the influence of admixtures on the properties of materials, different types of cement-based materials and alkali-activated cementitious materials show their own unique characteristics and laws.

For Portland cement-based materials, additives such as ethylene glycol, calcium chloride, calcium nitrate, and sodium nitrite can improve their low-temperature mechanical

properties to a certain extent. Especially in the negative temperature to positive temperature curing, the increase of ethylene glycol content significantly enhances the later strength of concrete, especially in the low-temperature conditions ( $-10\text{ }^{\circ}\text{C}$ ,  $-15\text{ }^{\circ}\text{C}$ ); the antifreeze effect is obvious. However, although some inorganic salt antifreeze can reduce frost heave deformation, it may aggravate residual deformation, which is consistent with the previous research conclusions.

In sulphoaluminate cement-based materials, the addition of styrene–butadiene emulsion under low-temperature curing is found to result in limited improvement in compressive strength and significant enhancement in flexural and tensile strengths. The content of lithium carbonate is proportional to the compressive strength within a certain range, and the combined addition of lithium carbonate and aluminum sulfate can improve the early and late compressive strength of the sulphoaluminate cement-based materials. However, retarders usually have adverse effects on the early strength of the sulphoaluminate cement-based materials, which further enriches the understanding of the performance changes of sulphoaluminate cement under the action of admixtures.

For alkali-activated cementitious materials, the addition of calcium oxide, sodium nitrate, and other admixtures can improve their low-temperature mechanical properties, especially at  $-10\text{ }^{\circ}\text{C}$  curing. Calcium oxide can improve the compressive and flexural strength of alkali-activated slag slurry. However, the research on the properties of alkali-activated cementitious materials with various inorganic salt admixtures (such as antifreeze, early strength, retarding, etc.) is still relatively scarce and needs further exploration.

Different types of cement-based materials and alkali-activated cementitious materials show different characteristics and influences in the use of admixtures under low-temperature conditions. The use of ethylene glycol and inorganic salt antifreeze enhances the performance of Portland cement under low temperatures. However, it also brings negative effects, such as residual deformation. Sulphoaluminate cement shows a positive effect of admixtures on flexural strength; however, the inhibition of retarder on early strength still needs to be further studied. However, research on admixtures of alkali-activated cementitious materials is relatively scarce, and it is urgent to explore the composite effects of different admixtures.

In general, although existing studies have revealed the positive effects of admixtures on different materials under low-temperature conditions, how to optimize the ratio of admixtures, select appropriate admixtures, and understand the changes in their long-term performance, which remain key areas for future research, is still a crucial focus. Especially in the practical engineering application of low-temperature curing, how to improve the durability and stability of concrete requires that the mechanism of action of admixtures and their interaction with cement-based materials or alkali-activated cementitious materials be discussed in depth so that more efficient and sustainable material design can be achieved.

## 5.2. *Effect of Admixtures on the Properties of Materials*

Under the condition of low temperatures, the research on the influence of admixtures on the properties of materials covers three aspects: industrial solid waste, nanomaterials, and hydrated calcium silicate seeds, which have their own characteristics and achievements.

In terms of industrial solid waste, under the same mix ratio and curing conditions, silica fume is more helpful in improving the compactness and final compressive strength of the cementitious system than fly ash. Silica fume can not only increase the final compressive strength but also optimize the pore size distribution of the system and reduce the porosity, thereby enhancing the frost resistance and chloride ion penetration resistance of concrete, which improves its overall durability.

In terms of nanomaterials, nano- $\text{CaCO}_3$ , nano- $\text{TiO}_2$ , and nano- $\text{SiO}_2$  have a certain influence on the mechanical properties and microstructure of materials under low-temperature curing. Nano- $\text{CaCO}_3$  can improve the early strength of concrete using a certain content. Nano- $\text{TiO}_2$  can refine the microstructure and improve the compressive strength of mortar under low temperatures. Nano- $\text{SiO}_2$  can repair some of the degraded pores and enhance the impermeability of cement paste. However, the optimum content and performance variation of nanomaterials at different low-temperature curing still need to be further clarified.

In terms of hydrated calcium silicate seed, hydrated calcium silicate can significantly improve the compressive strength of cement paste under low-temperature curing, promote the formation of hydration products, and refine the microstructure. For example, when cured at  $-5\text{ }^\circ\text{C}$ , 5% C-S-H can increase the peak value of hydration heat at the initial stage of cement paste, accelerate the formation of hydration products, and make the microstructure of the paste more dense.

Therefore, the selection and dosage of admixtures have a significant effect on the material properties under low-temperature curing. Silica fume and nano-materials can improve the early strength and frost resistance of concrete, but the ratio of admixtures still needs to be further optimized to ensure the best effect under low-temperature conditions. In addition, the mechanism of action of C-S-H is worthy of being further discussed, especially the practical application potential in low-temperature environments. On the whole, the study of admixtures under low-temperature conditions not only promotes the durability research of concrete but also provides a valuable reference for the design of concrete under low-temperature environments in practical engineering.

### *5.3. Relationship Between Pre-Curing Time and Material Properties*

Pre-curing measures can effectively reduce the frost heave deformation and residual deformation of concrete, and improve the frost resistance significantly. Studies have shown that prolonging the pre-curing time can increase the harmless pores of the sample, and it is more effective than simply adding antifreeze in inhibiting positive temperature settlement deformation. However, the relationship between the pre-curing time and the frost resistance critical strength is affected by many factors, such as curing temperature, material properties, and antifreeze types. Under different low-temperature curing temperatures, the optimal value of pre-curing time is different, and materials with higher strength grades usually require longer pre-curing time. This finding refines the relationship between pre-curing time and material properties, but further research is needed on the synergistic effect of pre-curing time and antifreeze components.

The influence of pre-curing time on material properties is also of great significance. The review results show that properly prolonging the pre-curing time can increase the harmless pores of the sample and improve the frost resistance of the material. However, it is not always beneficial when the pre-curing time is too long. For example, the strength of the cement mortar specimen reaches its highest When the pre-curing temperature is  $5\text{ }^\circ\text{C}$  and the pre-curing time is 400 min, longer pre-curing time does not further improve the strength. This indicates that there is a complex relationship between pre-curing time and material properties, and it is necessary to comprehensively consider factors such as curing temperature and material properties.

Materials have different requirements with different strength grades for pre-curing time. The higher the strength grade, the longer the pre-curing time is required. In practical engineering, it is necessary to determine the best pre-maintenance time through experiments according to specific materials and construction conditions. At the same time, the synergistic effect of pre-curing time and antifreeze components should also be given atten-

tion, and the combination of the two may further optimize the performance of the material at low temperatures. Future research can further explore the performance changes of different materials under different pre-curing times and antifreeze component combinations and provide more accurate prediction models for practical projects.

Future research should expand the scope of the investigation, explore the performance of various materials, admixtures, and additives, and optimize pre-curing measures to enhance the practical application value of the research results. Particularly in actual construction, how the pre-curing strategy can be flexibly adjusted according to different environmental conditions and material characteristics remains a problem that is worthy of further discussion.

#### 5.4. Outlook

Future research can further explore the optimization and synergistic effects of antifreeze components, admixtures, and pre-curing measures under low-temperature conditions. While current studies have revealed the impact of individual factors on concrete performance; however, more experimental and theoretical support is needed to improve the freeze resistance, durability, and long-term performance of materials using proper mixing ratios and combined applications. Additionally, the optimization of pre-curing time and the synergistic effects of antifreeze agents should be further investigated to enhance material performance in different low-temperature environments, providing more precise guidance for practical engineering applications.

### 6. Conclusions and Recommendations

Under conditions of low-temperature curing in winter, the setting rate of materials decreases, the hydration process is hindered, and strength degradation becomes inevitable. This paper primarily collects and organizes the research findings on cement-based materials under low-temperature curing from recent years, introducing the research status of antifreeze components, nanoparticles, and pre-curing measures to enhance the mechanical properties and micro-mechanisms of materials under low-temperature curing. The three methods are summarized, and suggestions for subsequent development are provided.

- (1) Various types of antifreeze early strength components are used with ordinary Portland cement-based materials, including calcium chloride, sodium nitrite, calcium nitrate, ethylene glycol, and triethanolamine, which have shown better effects. It is worth noting that existing data vary in maintenance ages, and the urgency to determine whether the compressive strength measured at the curing age of  $-7 + 28$  days is representative of different materials and field environments as a unified evaluation system. Future research should progressively consider the influence of incorporating single and composite antifreeze components at low temperatures on the performance of new materials, such as ultra-high-performance concrete and alkali-activated materials.
- (2) Sulfoaluminate cement and magnesium phosphate cement-based materials strengthen quickly and early. Additionally, their performance at room temperature is already very superior, and the incorporation of antifreeze components can play a strengthening role under low-temperature curing conditions. However, magnesium phosphate cement has a high production cost and is more suitable as a rapid repair material at low temperatures.
- (3) Alkali-activated cementitious materials, utilizing industrial solid waste, exhibit superior performance and are considered alternatives to ordinary Portland cement. However, research in this area has started late, and due to the choice of precursor and activator ratios, research findings are limited and scattered, lacking a systematic structural system. Future studies should not only examine the performance of alkali-

activated cementitious materials under low-temperature conditions but also focus on their long-term comprehensive performance, establishing a diversified index performance evaluation system. The relevant standards and procedures for alkali-activated materials should be formulated promptly.

- (4) The mineral admixtures when studying admixtures are mainly fly ash and silica fume. Silica fume has a better low-temperature improvement effect than fly ash under identical conditions. The incorporation of nano-materials and hydrated calcium silicate seeds has contributed to physically filling and refining the pores of the slurry, reducing material porosity, mitigating the impact of freezing damage at low temperatures, and improving the later strength. The selection of beneficial admixtures should aim to make rational use of industrial solid waste, adhere to the dual-carbon strategy, respond to the United Nations' call for zero carbon, and promote the green development of the construction industry.
- (5) The length of pre-curing time varies according to the different strength grades of concrete; higher strength grades necessitate longer pre-curing times. After experimental research on different materials and strength grades, various pre-curing methods are analyzed, and later evaluation methods are considered to accurately predict the critical strength of concrete frost resistance for different materials. This is combined with pre-curing methods such as temperature storage and greenhouse methods, allowing for more scientific, reasonable, and economical determination of pre-curing time, resource conservation, and environmental protection. The combination of pre-curing and antifreeze component measures indicates a need for further research to explore whether a complementary effect exists between the two under different materials, as well as to determine the optimal pre-curing time, select antifreeze components, and ascertain the appropriate dosages.
- (6) For new composite materials, new high-strength cement-based materials, alkali-activated cementitious materials, and geopolymers concrete, the late start of research and the multitude of influencing factors necessitate accelerated research efforts by scholars. Combined with engineering practice, the mechanical properties and durability of materials under low-temperature curing are studied, which can allow high-efficiency materials to be applied in practical engineering as soon as possible. Moreover, based on the test results, combining test data with numerical analysis to establish an intelligent prediction model through artificial neural networks and machine learning methods will guide engineering practices scientifically, efficiently, and conveniently, providing a reference for the safety, durability, and economic design of the structure under low-temperature curing in winter.

**Author Contributions:** X.Y.: conceptualization, supervision, validation, writing—review and editing. M.W.: data curation, writing—original draft, formal analysis, visualization. Y.Z.: formal analysis, writing—review and editing. L.N.: supervision, formal analysis. X.J.: fund providers. S.C.: fund providers, formal analysis. W.H.: supervision, formal analysis. L.H.: fund providers, formal analysis. All authors have read and agreed to the published version of the manuscript.

**Funding:** This project was sponsored by the Joint Fund of Henan Province Science and Technology R&D Program (225200810056, 235200810044), Key Research and Development Project of Henan Province (242102241019), Key Research Project of Institutions of Higher Education in Henan Province (25CY005), North China University of Water Resources and Electric Power Graduate student innovation project (NCWUYC202416048, NCWUYC202416049). This study was supported by Shengqiang Chen (No. 225200810056, 235200810044), Xiaoxiang Ji (No. 242102241019, 25CY005), Mingduo Wan (No. NCWUYC202416048) and Linyan Han (No. NCWUYC202416049). And The APC was funded by [No. 225200810056].



**Conflicts of Interest:** Author Yongsheng Zhu was employed by the company Northeast Branch China Construction Eighth Engineering Division Co., Ltd. Author Shengqiang Chen was employed by the company Henan Building Materials Research and Design Institute Co., Ltd. The remaining authors declare that the research was conducted in the absence of any commercial or financial relationships that could be construed as a potential conflict of interest.

## References

- Lothenbach, B.; Winnefeld, F.; Alder, C.; Wieland, E. Effect of temperature on the pore solution, microstructure and hydration products of Portland cement pastes. *Cem. Concr. Res.* **2007**, *37*, 483–491. [\[CrossRef\]](#)
- Alzaza, A.; Ohenoja, K.; Dabbabi, R.; Illikainen, M. Enhancing the hardened properties of blended cement paste cured at 0 °C by using alkali-treated ground granulated blast furnace slag. *Cem. Concr. Compos.* **2022**, *134*, 104757. [\[CrossRef\]](#)
- Çullu, M.; Arslan, M. The effects of antifreeze use on physical and mechanical properties of concrete produced in cold weather. *Compos. Part B Eng.* **2013**, *50*, 202–209. [\[CrossRef\]](#)
- Zhao, W.; Wang, M.H.; Chen, C.B.; Huang, L.M. Variations, controls and predictions of soil saturated hydraulic conductivity under different land use types in the alpine region of Tibet, China. *Geoderma Reg.* **2023**, *35*, e00723. [\[CrossRef\]](#)
- Zhang, T.; Tian, S.; Chen, H.Y.; Zhou, Y.L. Recent advances in concrete winterisation technology in the last two decades. *Concrete* **2013**, 40–42. (In Chinese)
- Lu, J.G.; Liu, J.N.; Yang, H.H.; Gao, J.J.; Wan, X.S. Influence of curing temperatures on the performances of fiber-reinforced concrete. *Constr. Build. Mater.* **2022**, *339*, 127640. [\[CrossRef\]](#)
- Jiang, Z.W.; He, B.; Zhu, X.P.; Ren, Q.; Zhang, Y. State-of-the-art review on properties evolution and deterioration mechanism of concrete at cryogenic temperature. *Constr. Build. Mater.* **2020**, *257*, 11945–11946. [\[CrossRef\]](#)
- Zhang, H.Z.; Ai, J.H.; Ren, Q.; ZHU, X.P.; He, B.; Jiang, Z.W. Understanding the strength evolution of alkali-activated slag pastes cured at subzero temperature. *Cem. Concr. Compos.* **2023**, *138*, 104993. [\[CrossRef\]](#)
- Zhang, G.; Yang, H.L.; Cheng, J.; Yang, Y.Z. Novel selection of environment-friendly cementitious materials for winter construction: Alkali-activated slag/Portland cement. *J. Clean. Prod.* **2020**, *258*, 120592. [\[CrossRef\]](#)
- Yang, H.; Wang, H.L.; Li, J.S.; Zhang, Z.R.; Huang, X.; XUE, Q. Strength evolution and microstructure of alkali-activated ultra-fine slag in low-temperature environments. *Constr. Build. Mater.* **2024**, *435*, 136852. [\[CrossRef\]](#)
- Yang, K.; Yang, C.; Zhang, J. First structural use of site-cast, alkali-activated slag concrete in China. *Proc. Inst. Civ. Eng.-Struct. Build.* **2018**, *171*, 800–809. [\[CrossRef\]](#)
- Zhang, Z.; Sun, Q.S.; Yue, X.L.; Sun, Z.L.; Liu, Y.C. Temperature field analysis and prediction of winter construction warm shed method based on hot air heating. *Case Stud. Therm. Eng.* **2024**, *60*, 104709. [\[CrossRef\]](#)
- Shi, T.; Deng, C.; Zhao, J.; Ding, P.X.; Fan, Z.H. Temperature field of concrete cured in winter conditions using thermal control measures. *Adv. Mater. Sci. Eng.* **2022**, *2022*, 7255601. [\[CrossRef\]](#)
- Xu, Z.; Yu, H.L.; Sun, X.J.; Zhao, M.; Hui, D. Research on mechanical properties and microscopic mechanism of multi-based geopolymer concrete under combined action of pre-curing and nano-silica. *J. Build. Eng.* **2024**, *97*, 110930. [\[CrossRef\]](#)
- Zhu, W.Z.; Shang, X.L. Understanding and practice of some concepts of frost critical strength of concrete in winter construction. *Constr. Technol.* **1995**, 30–33. (In Chinese)
- Koniorczyk, M.; Bednarska, D.; Omrani, I.A.N.; Wieczorek, A.; Gong, F. On Water Freezing in Slag-Blended Cementitious Materials at Early Ages. *J. Build. Eng.* **2024**, *92*, 109778. [\[CrossRef\]](#)
- Mobili, A.; Telesca, A.; Marroccoli, M.; Tittarelli, F. Calcium sulfoaluminate and alkali-activated fly ash cements as alternative to Portland cement: Study on chemical, physical-mechanical, and durability properties of mortars with the same strength class. *Constr. Build. Mater.* **2020**, *246*, 118436. [\[CrossRef\]](#)
- Zhang, Q.S.; Cao, X.; Ma, R.; Sun, S.; Fang, L.; Lin, J.; Luo, J. Solid waste-based magnesium phosphate cements: Preparation, performance and solidification/stabilization mechanism. *Constr. Build. Mater.* **2021**, *297*, 123761. [\[CrossRef\]](#)
- Zhang, L.H.; Lu, Z.C.; Zhang, Y.R. New insight into the combined effect of aluminum sulfate and triethanolamine on cement hydration. *Cem. Concr. Res.* **2024**, *181*, 107547. [\[CrossRef\]](#)
- Liu, Z.; Lou, B.; Barbieri, D.M.; Sha, A.; Ye, T.; Li, Y. Effects of pre-curing treatment and chemical accelerators on Portland cement mortars at low temperature (5 °C). *Constr. Build. Mater.* **2020**, *240*, 117893. [\[CrossRef\]](#)
- Zhang, L.F.; Ma, R.; Lai, J.Y.; Ruan, S.Q.; Qian, X.Q.; Yan, D.M. Performance buildup of concrete cured under low-temperatures: Use of a new nanocomposite accelerator and its application. *Constr. Build. Mater.* **2022**, *335*, 127529. [\[CrossRef\]](#)
- Zhao, Y.S.; Zhao, Y.X.; Zhu, Z.H.; Chen, G.F.; Wu, H.X.; Liu, C.; Gao, J.M. Effect of a novel negative temperature early-strength agent in improving concrete performance under varying curing temperatures. *Case Stud. Constr. Mater.* **2024**, *21*, e03748. [\[CrossRef\]](#)

23. Zhang, B.; Zhu, H.; Feng, P.; Zhang, P. A review on shrinkage-reducing methods and mechanisms of alkaliactivated/geopolymer systems: Effects of chemical additives. *J. Build. Eng.* **2022**, *49*, 104056. [\[CrossRef\]](#)
24. Kothari, A.; Habermehl-Cwirzen, K.; Hedlund, H.; Cwirzen, A. A Review of the Mechanical Properties and Durability of Ecological Concretes in a Cold Climate in Comparison to Standard Ordinary Portland Cement-Based Concrete. *Materials* **2020**, *13*, 3467. [\[CrossRef\]](#) [\[PubMed\]](#)
25. Wang, Y.F.; Lei, L.; Liu, J.H.; Ma, Y.H.; Liu, Y.; Xiao, Z.Q.; Shi, C.J. Accelerators for normal concrete: A critical review on hydration, microstructure and properties of cement-based materials. *Cem. Concr. Compos.* **2022**, *134*, 104762. [\[CrossRef\]](#)
26. JC 475-2004; National Development and Reform Commission of the People's Republic of China. Antifreeze for Concrete. China Building Material Industry Press: Beijing, China, 2004. (In Chinese)
27. Liu, R.Q.; Liu, J.; Liu, Y.; Zhou, H.H. Influence of freezing environment on freezing critical strength of low-temperature concrete. *J. Liaoning Tech. Univ.* **2011**, *30*, 92–95. [\[CrossRef\]](#)
28. Jiang, S.H.; Dong, S.H.; Zhu, W.Z.; Li, H.B.; Yin, S.H. Research on critical strength of negative temperature concrete subjected to freezing based on frost resistance. *China Concr. Cem. Prod.* **2019**, 8–10. (In Chinese) [\[CrossRef\]](#)
29. Jiang, S.H.; Dong, S.H.; Zhu, W.Z.; Li, H.B.; Yin, S.H. Research on critical strength of negative temperature concrete subjected to freezing based on compressive strength. *China Concr. Cem. Prod.* **2019**, 24–26. (In Chinese) [\[CrossRef\]](#)
30. Jiang, C.H.; Yang, Y.; Wang, Y.; Zhou, Y.N.; Ma, C.C. Autogenous shrinkage of high performance concrete containing mineral admixtures under different curing temperatures. *Constr. Build. Mater.* **2014**, *61*, 260–269. [\[CrossRef\]](#)
31. Velay-Lizancos, M.; Martinez-Lage, I.; Azenha, M.; Vázquez-Burgo, P. Influence of temperature in the evolution of compressive strength and in its correlations with UPV in eco-concretes with recycled materials. *Constr. Build. Mater.* **2016**, *124*, 276–286. [\[CrossRef\]](#)
32. Wang, X.P.; Zhang, R.L.; Duan, Y.; Guo, H.Z.; Zhang, J.W. Effect of mould entry temperature on the heat of hydration of cement under continuous negative temperature and its prediction model. *Acta Mater. Compos. Sin.* **2022**, *39*, 4718–4731. (In Chinese) [\[CrossRef\]](#)
33. Zhang, W.Y.; Nie, S.; Xu, M.F.; Zhou, J.; Li, H. Progress of activation of high Baileyite sulphoaluminate cement. *Bull. Chin. Ceram. Soc.* **2022**, *41*, 2979–2992. (In Chinese) [\[CrossRef\]](#)
34. Shen, Y.; Zhang, W.; Chen, X.; Li, X.P. Research progress of sulphoaluminate cement modification. *Bull. Chin. Ceram. Soc.* **2019**, *38*, 683–687. (In Chinese) [\[CrossRef\]](#)
35. Liu, J.; Lu, R.H.; Zhang, Z.Q. Research Progress on Properties of Magnesium Phosphate Cement. *Mater. Rep.* **2021**, *35*, 23068–23075. (In Chinese)
36. Haque, M.A.; Chen, B. Research progresses on magnesium phosphate cement: A review. *Constr. Build. Mater.* **2019**, *211*, 885–898. [\[CrossRef\]](#)
37. Nodehi, M.; Taghvaei, V.M. Alkali-Activated Materials and Geopolymer: A Review of Common Precursors and Activators Addressing Circular Economy. *Circ. Econ. Sustain.* **2022**, *2*, 165–196. [\[CrossRef\]](#)
38. Gökçe, H.S.; Tuyan, M.; Nehdi, M.L. Alkali-activated and geopolymer materials developed using innovative manufacturing techniques: A critical review. *Constr. Build. Mater.* **2021**, *303*, 124483. [\[CrossRef\]](#)
39. Tan, H.B.; Li, M.G.; Ren, J.; Deng, X.F.; Zhang, X.; Nie, K.J.; Zhang, J.J.; Yu, Z.Q. Effect of aluminum sulfate on the hydration of tricalcium silicate. *Constr. Build. Mater.* **2019**, *205*, 414–424. [\[CrossRef\]](#)
40. Hoang, K.; Justnes, H.; Geiker, M. Early age strength increase of fly ash blended cement by a ternary hardening accelerating admixture. *Cem. Concr. Res.* **2016**, *81*, 59–69. [\[CrossRef\]](#)
41. Hirsch, T.; Lu, Z.; Stephan, D. Effect of different sulphate carriers on Portland cement hydration in the presence of triethanolamine. *Constr. Build. Mater.* **2021**, *294*, 123528. [\[CrossRef\]](#)
42. Lu, Z.C.; Kong, X.M.; Jansen, D.; Zhang, C.Y.; Wang, J.; Pang, X.F.; Yin, J.H. Towards a further understanding of cement hydration in the presence of triethanolamine. *Cem. Concr. Res.* **2020**, *132*, 106041. [\[CrossRef\]](#)
43. Liu, Y.P.; Yang, S.; Li, J.H.; Wang, F.Z.; Hu, S.G. Effect of w/c ratio and antifreeze admixture on the frost damage of sulfoaluminate cement concrete at  $-20^{\circ}\text{C}$ . *Constr. Build. Mater.* **2022**, *347*, 128457. [\[CrossRef\]](#)
44. Nmai, C.K. Cold weather concreting admixtures. *Cem. Concr. Compos.* **1998**, *20*, 121–128. [\[CrossRef\]](#)
45. Cheung, J.; Jeknavorian, A.; Roberts, L.; Silva, D. Impact of admixtures on the hydration kinetics of Portland cement. *Cem. Concr. Res.* **2011**, *41*, 1289–1309. [\[CrossRef\]](#)
46. Marchon, D.; Kawashima, S.; Bessaies-Bey, H.; Mantellato, S.; Ng, S. Hydration and rheology control of concrete for digital fabrication: Potential admixtures and cement chemistry. *Cem. Concr. Res.* **2018**, *112*, 96–110. [\[CrossRef\]](#)
47. Chaves Figueiredo, S.; Çopuroğlu, O.; Schlangen, E. Effect of viscosity modifier admixture on Portland cement paste hydration and microstructure. *Constr. Build. Mater.* **2019**, *212*, 818–840. [\[CrossRef\]](#)
48. Nwankwo, C.O.; Bamigboye, G.O.; Davies, I.E.E.I.; Michaels, T.A. High volume Portland cement replacement: A review. *Constr. Build. Mater.* **2020**, *260*, 120445. [\[CrossRef\]](#)

49. Yang, Y.Z.; Gao, X.J.; Deng, H.G.; Ba, H.J. Non-destructive monitoring of internal structural development of negative temperature concrete. *J. Harbin Inst. Technol.* **2009**, *41*, 43–47. (In Chinese)
50. Zhang, L.; Li, X. Research on special antifreeze agent for BFJ polycarboxylic acid high-efficiency water reducing agent. *Concrete* **2011**, 88–89. (In Chinese)
51. Zhou, M.R.; Zhang, H.J.; Zhang, J.; Long, L.J. Evaluation method and application research of compound antifreeze. *Concrete* **2012**, 78–80. (In Chinese)
52. Wang, J.L.; Sun, X.B.; Yang, Z.F. Research on the effect of antifreeze components on the properties of cement concrete. *Bull. Chin. Ceram. Soc.* **2014**, *33*, 3331–3337. (In Chinese) [[CrossRef](#)]
53. Song, D.S.; Dai, M.; Gai, Y.F.; Zhang, J.L.; Xin, Y.L. Influence of antifreeze components on the properties of negative temperature concrete. *Concrete* **2011**, 55–56+61. (In Chinese)
54. Yin, M.; Bai, H.T.; Zhou, L. Experimental study on the determination of antifreeze admixture for negative temperature concrete. *Sci. Technol. Eng.* **2014**, *14*, 290–294. (In Chinese)
55. Karagoel, F.; Demirboga, R.; Kaygusuz, M.A.; Yadollahi, M.M.; Polatet, R. The influence of calcium nitrate as antifreeze admixture on the compressive strength of concrete exposed to low temperatures. *Cold Reg. Sci. Technol.* **2013**, *89*, 30–35. [[CrossRef](#)]
56. Demirboğa, R.; Karagöl, K.; Polat, R.; Kaygusuzet, M.A. The effects of urea on strength gaining of fresh concrete under the cold weather conditions. *Constr. Build. Mater.* **2014**, *64*, 114–120. [[CrossRef](#)]
57. Jia, B.X.; Li, Q.W.; Liang, P.F.; Li, G.X. Research on the effect of antifreeze on the mechanical properties of spontaneous combustion gangue concrete. *Non-Met. Mines* **2016**, *39*, 68–71. (In Chinese)
58. Reddy, P.N.; Naqash, J.A. Effect of Antifreeze Admixtures on Cold Weather Concrete. *Int. J. Eng.* **2019**, *32*, 366–372.
59. Zhang, G.; Yu, H.Y.; Li, H.M.; Yang, Y.Z. Experimental study of deformation of early age concrete suffering from frost damage. *Constr. Build. Mater.* **2019**, *215*, 410–421. [[CrossRef](#)]
60. Skripkiunas, G.; Kicaite, A.; Justnes, H.; Pundienė, I. Effect of Calcium Nitrate on the Properties of Portland-Limestone Cement-Based Concrete Cured at Low Temperature. *Materials* **2021**, *14*, 1611. [[CrossRef](#)]
61. Karagol, F.; Demirboga, R.; Khushefati, W.H. Behavior of fresh and hardened concretes with antifreeze admixtures in deepfreeze low temperatures and exterior winter conditions. *Constr. Build. Mater.* **2015**, *76*, 388–395. [[CrossRef](#)]
62. Khan, J.; Kumar, G.S. Influence of binary antifreeze admixtures on strength performance of concrete under cold weather conditions. *J. Build. Eng.* **2021**, *34*, 102055. [[CrossRef](#)]
63. Dong, S.H.; Feng, C.F.; Jiang, S.H.; Zhu, W.Z. Effect of freezing temperature on the microstructure of negative temperature concrete. *Adv. Mater. Res.* **2013**, *663*, 343–348. [[CrossRef](#)]
64. Hu, Y.B.; Miao, G.Y.; Yu, X. Research on mechanical properties and hydration characteristics of concrete under negative temperature environment. *J. Build. Mater.* **2017**, *20*, 975–980. (In Chinese)
65. Thomas, J.J.; Allen, A.J.; Jennings, H.M. Hydration Kinetics and Microstructure Development of Normal and CaCl<sub>2</sub>-Accelerated Tricalcium Silicate Pastes. *J. Phys. Chem. C* **2009**, *113*, 19836–19844. [[CrossRef](#)]
66. Tao, Y.X.; Rahul, A.V.; Mohan, M.K.; De, S.G.; Van, T.K. Recent progress and technical challenges in using calcium sulfoaluminate (CSA) cement. *Cem. Concr. Compos.* **2023**, *137*, 104908. [[CrossRef](#)]
67. Ke, G.J.; Zhang, J.; Liu, Y. Shrinkage characteristics of calcium sulphoaluminate cement concrete. *Constr. Build. Mater.* **2022**, *337*, 127627. [[CrossRef](#)]
68. Li, M. Research on Hydration Characteristics of Sulphoaluminate Cement Under Low Temperature Environment. Master's Thesis, Beijing Institute of Technology, Beijing, China, 2020. (In Chinese).
69. Wang, P.M.; Li, N.; Xu, L.L.; Zhang, G.F. Hydration process and strength development of sulphoaluminate cement under low temperature maintenance. *J. Chin. Ceram. Soc.* **2017**, *45*, 242–248. (In Chinese) [[CrossRef](#)]
70. Wang, R.; Xu, Y.D. Effect of curing temperature on the physical and mechanical properties of butylbenzene emulsion/sulphoaluminate cement mortar. *J. Chin. Ceram. Soc.* **2017**, *45*, 227–234. (In Chinese) [[CrossRef](#)]
71. Wang, R.; Zhang, T. Drying shrinkage of styrene-butadiene emulsion/sulphoaluminate cement mortar at different temperature and humidity. *J. Build. Mater.* **2018**, *21*, 768–774. (In Chinese)
72. Wang, J.Y.; Ye, J.Y.; Cheng, H.; Shi, D.; Ren, J.R.; Zhang, W.S. Effect of retarder on hydration and strength of fasthardening sulphoaluminate cement at minus 10 °C. *J. Chin. Ceram. Soc.* **2020**, *48*, 1285–1294. (In Chinese) [[CrossRef](#)]
73. Wang, Z.P.; Zhao, Y.T.; Xu, L.L. Hydration characteristics of sulphoaluminate cement under different maintenance temperatures. *J. South China Univ. Technol.* **2018**, *46*, 30–38. (In Chinese)
74. Li, G.X.; Zhang, J.; Song, Z.; Shi, C.; Zhang, A. Improvement of workability and early strength of calcium sulphoaluminate cement at various temperature by chemical admixtures. *Constr. Build. Mater.* **2018**, *160*, 427–439. [[CrossRef](#)]
75. Liu, Y.P.; Li, J.H.; Yang, C.; Liu, Z.C. Influence of antifreeze and early-strengthening agent on the negative temperature hydration property of sulphoaluminate cement. *Bull. Chin. Ceram. Soc.* **2021**, *40*, 359–367. (In Chinese) [[CrossRef](#)]
76. Wang, W.B. Effect of lithium carbonate on hydration and properties of sulphoaluminate cement under low temperature environment. *New Build. Mater.* **2019**, *46*, 54–57. (In Chinese)

77. Wang, P.M.; Li, N.; Xu, L.L. Hydration evolution and compressive strength of calcium sulphoaluminate cement constantly cured over the temperature range of 0 to 80 °C. *Cem. Concr. Res.* **2017**, *100*, 203–213. [\[CrossRef\]](#)
78. Zhang, H.F.; Ye, J.Y.; Ren, J.R.; Yang, C.S.; Zhang, W.S.; Shi, D.; Zhang, J.T. Effect of calcium chloride solution on the properties of sulphoaluminate cement at −10 °C. *J. Chin. Ceram. Soc.* **2022**, *50*, 2834–2843. (In Chinese)
79. Jia, X.W.; Luo, J.Y.; Zhang, W.X.; Qian, S.H.; Li, J.M. Preparation and Application of Self-Curing Magnesium Phosphate Cement Concrete with High Early Strength in Severe Cold Environments. *Materials* **2020**, *13*, 5587. [\[CrossRef\]](#)
80. Jia, X.W.; Lian, L.; To, J.; Tu, H.; Hou, T.J.; Wang, P. Effect of magnesium oxide whiskers on the early mechanical properties of magnesium phosphate cement under severe cold environment. *J. Funct. Mater.* **2021**, *52*, 12030–12035. (In Chinese)
81. Yi, H.H.; Zhang, Y.; Lu, J.B.; Li, D.X. Study on the failure of magnesium phosphate cement under low temperature. *Bull. Chin. Ceram. Soc.* **2014**, *33*, 197–201. (In Chinese)
82. Jia, X.W.; Li, J.M.; Wang, P.; Qian, J.S.; Tang, M.H. Preparation and mechanical properties of magnesium phosphate cement for rapid construction repair in ice and snow. *Constr. Build. Mater.* **2019**, *229*, 116921–116927. [\[CrossRef\]](#)
83. Jia, X.W.; Luo, J.Y.; Zhang, W.X.; Tang, M.H.; Qian, J.S. Reaction characteristics and compressive strength of magnesia-phosphate cement at negative temperatures. *Constr. Build. Mater.* **2021**, *305*, 124819. [\[CrossRef\]](#)
84. Yuan, J.; Zhang, Z.C.; Chen, X.; Pan, Z.; Huang, X. Study on early mechanical properties of icewater blended magnesium phosphate cement in cold environment. *Concrete* **2022**, *8*, 10–14. (In Chinese)
85. Yuan, J.; Huang, X.; Chen, X.; Ge, Q.; Zhang, Z.C. Early-age mechanical properties and hydration degrees of magnesium phosphate cement paste in freezing winter of cold regions. *Constr. Build. Mater.* **2022**, *345*, 128337. [\[CrossRef\]](#)
86. Habert, G.; De Lacaillerie, D.E.; Roussel, N. An environmental evaluation of geopolymer based concrete production: Reviewing current research trends. *J. Clean. Prod.* **2011**, *19*, 1229–1238. [\[CrossRef\]](#)
87. Burciaga-Díaz, O.; Escalante-García, J.I. Strength and durability in acid media of alkali silicate-activated metakaolin geopolymers. *J. Am. Ceram. Soc.* **2012**, *95*, 2307–2313. [\[CrossRef\]](#)
88. Justnes, H.; Kim, M.O.; Ng, S.; Qian, X. Methodology of calculating required chloride diffusion coefficient for intended service life as function of concrete cover in reinforced marine structures. *Cem. Concr. Compos.* **2016**, *73*, 316–323. [\[CrossRef\]](#)
89. Yang, G.J.; Wang, Z.Y. Durability properties of sustainable alkali-activated cementitious materials as marine engineering material: A review. *Mater. Today Sustain.* **2022**, *17*, 100099. [\[CrossRef\]](#)
90. Akinyemi, B.A.; Alaba, P.A.; Rashedi, A. Selected performance of alkali-activated mine tailings as cementitious composites: A review. *J. Build. Eng.* **2022**, *50*, 104154. [\[CrossRef\]](#)
91. Wei, X.B.; Li, D.Q.; Ming, F.; Yang, C.S.; Chen, L. Influence of Low-Temperature Curing on the Mechanical Strength, Hydration Process, and Microstructure of Alkali-Activated Fly Ash and Ground Granulated Blast Furnace Slag Mortar. *Constr. Build. Mater.* **2021**, *269*, 121811. [\[CrossRef\]](#)
92. Huang, X.; Mao, H.Y.; Yuan, X.F.; Yang, Y. Study on the properties of alkali slag cement at −20 °C. *Bulletin of the Chinese Ceramic Society* **2014**, *33*, 2052–2055. (In Chinese) [\[CrossRef\]](#)
93. Ju, C.; Liu, Y.S.; Jia, M.J.; Yu, K.; Yu, Z.; Yang, Y. Effect of calcium oxide on mechanical properties and microstructure of alkali-activated slag composites at subzero temperature. *J. Build. Eng.* **2020**, *32*, 101561. [\[CrossRef\]](#)
94. Yang, K.; Yang, Y.; Deng, J.X.; Xiong, D.Y.; Zhu, X.H. Using calcium-rich precursors to improve the early-compressive strength of alkali-activated slag cement at low temperature. *Struct. Concr.* **2022**, *23*, 2221–2232. [\[CrossRef\]](#)
95. Chen, T.; Ren, B.; Wang, Z.H.; Meng, X.; Ning, Y.P.; Lv, Y. Effect of early strength agent on the hydration of geopolymer mortar at low temperatures. *Case Stud. Constr. Mater.* **2022**, *17*, e01419. [\[CrossRef\]](#)
96. Alzaza, A.; Ohenoja, K.; Illikainen, M. Onepart alkali-activated blast furnace slag for sustainable construction at subzero temperatures. *Constr. Build. Mater.* **2021**, *276*, 122026. [\[CrossRef\]](#)
97. Bai, S.; Guan, X.C.; Li, G.Y. Effect of the early age frost damage and nano-SiO<sub>2</sub> modification on the properties of Portland cement paste. *Constr. Build. Mater.* **2020**, *262*, 120098. [\[CrossRef\]](#)
98. Ogawa, Y.; Uji, K.; Ueno, A.; Kawai, K. Contribution of fly ash to the strength development of mortars cured at different temperatures. *Constr. Build. Mater.* **2021**, *276*, 122191. [\[CrossRef\]](#)
99. Alzaza, A.; Ohenoja, K.; Langås, I.; Arntsen, B.; Poikelispää, M.; Illikainen, M. Low-temperature (−10 °C) curing of Portland cement paste—Synergetic effects of chloride-free antifreeze admixture, C–S–H seeds, and room-temperature pre-curing. *Cem. Concr. Compos.* **2022**, *125*, 104319. [\[CrossRef\]](#)
100. Lv, Y.; Bai, E.L.; Wang, Z.H.; Meng, X.; Sun, H.Y. Experimental and microscopic study on the preparation of silica fume-metakaolin-slag base polymer mortar at low temperature. *Mater. Rep.* **2023**, *37*, 218–226. (In Chinese)
101. Yang, Z.B.; Liu, Y.; Chen, Q.R.; Tang, J.S.; Zhu, B.Q.; Zhu, X.K. Mechanism of ultrafine mineral admixture for concrete. *Mater. Rep.* **2023**, *37*, 151–155. (In Chinese)
102. Zhao, Y.M.; Zhang, Z.; Wang, P.; Zhang, M.F. Influence of mineral dopants on the properties of UHPC. *Bull. Chin. Ceram. Soc.* **2022**, *41*, 3170–3175. (In Chinese)



103. Yang, Y.Z.; Ba, H.J. Interfacial microstructure and properties of negative temperature antifreeze concrete. *J. Chin. Ceram. Soc.* **2007**, *1125*–1130. (In Chinese)
104. He, X.X.; Kong, L.Z.; Zhou, S. Experimental study on compressive properties of fly ash concrete prisms with low-temperature curing. *Build. Struct.* **2020**, *50*, 38–43. (In Chinese)
105. Liu, L.; Li, Y.; Ouyang, P.; Yang, Y.Q. Hydration of the silica fume-Portland cement binary system at lower temperature. *Constr. Build. Mater.* **2015**, *93*, 919–925. [[CrossRef](#)]
106. Jun, L.; Li, Y.; Yang, Y.Q.; Cui, Y.P. Effect of Low Temperature on Hydration Performance of the Complex Binder of Silica Fume-Portland Cement. *J. Wuhan Univ. Technol.* **2014**, *29*, 75–81.
107. Bai, S.; Yu, L.B.; Guan, X.C.; Li, H.; Ou, J.P. Study on the long-term chloride permeability of nano-silica modified cement pastes cured at negative temperature. *J. Build. Eng.* **2022**, *57*, 104854. [[CrossRef](#)]
108. Feng, J.H.; Yang, F.; Qian, S.Z. Improving the bond between polypropylene fiber and cement matrix by nano calcium carbonate modification. *Constr. Build. Mater.* **2021**, *269*, 121249. [[CrossRef](#)]
109. Francioso, V.; Moro, C.; Martinez-Lage, I.; Velay-Lizancos, M. Curing temperature: A key factor that changes the effect of TiO<sub>2</sub> nanoparticles on mechanical properties, calcium hydroxide formation and pore structure of cement mortars. *Cem. Concr. Compos.* **2019**, *104*, 103374. [[CrossRef](#)]
110. Xu, Q.; Meng, T.; Huang, M. Effects of Nano-CaCO<sub>3</sub> on the Compressive Strength and Microstructure of High Strength Concrete in Different Curing Temperature. *Appl. Mech. Mater.* **2011**, *121*, 126–131.
111. Skoczylas, K.; Rucińska, T. The effects of low curing temperature on the properties of cement mortars containing nanosilica. *Nanotehnologii V Stroitu*. **2019**, *11*, 536–544. [[CrossRef](#)]
112. Tang, S.W.; Wang, Y.; Geng, Z.C.; Xu, X.F.; Yu, W.Z.; Hu, B.A.; Chen, J.T. Structure, Fractality, Mechanics and Durability of Calcium Silicate Hydrates. *Fractal Fract.* **2021**, *5*, 47. [[CrossRef](#)]
113. Zhang, H.; Tian, X.; Gu, X.; Zhang, Q. Simulation of free water freezing with hydrated calcium silicate pore water based on coarse-grained molecular dynamics. *Chin. J. Comput. Mech.* **2024**, *41*, 194–201. (In Chinese)
114. Zhang, G.; Yang, Y.Z.; Li, H.M. Calcium-silicate-hydrate seeds as an accelerator for saving energy in cold weather concreting. *Constr. Build. Mater.* **2020**, *264*, 120191. [[CrossRef](#)]
115. Zheng, X.G.; Yu, P.Y.; Duan, L.F.; Li, S.M.; Zhang, C.; Deng, Q.S. Effect of hydrated calcium silicate crystal species on compressive strength of concrete under negative temperature curing. *Railw. Eng.* **2022**, *62*, 150–153. (In Chinese)
116. Alzaza, A.; Ohenoja, K.; Ahmed Shaikh, F.U.; Illikainen, M. Mechanical and durability properties of C–S–H-seeded cement mortar cured at fluctuating low temperatures with granulated blast furnace slag as fine aggregates. *J. Build. Eng.* **2022**, *57*, 104879. [[CrossRef](#)]
117. *GBJ 204-1983*; Specification for Construction and Acceptance of Reinforced Concrete Works. China Building Industry Press: Beijing, China, 1983. (In Chinese)
118. Huang, S.Y.; Wu, C.S. Several controversial issues in winter concrete construction. *Low Temp. Archit. Technol.* **1990**, 38–40. (In Chinese)
119. Xiang, Z.X. Study on the freezing critical strength of negative temperature concrete. *Archit. Technol.* **1988**, 2–8. (In Chinese)
120. Song, X.T. Discussion on the critical strength of concrete with antifreeze. *Low Temp. Archit. Technol.* **1989**, 20–22. (In Chinese)
121. Qu, Z.Z. Critical strength of concrete before freezing. *Constr. Technol.* **1988**, 59–60. (In Chinese)
122. Zhao, Y.Y. Early allowable freezing critical strength of antifreeze-added concrete. *Ind. Constr.* **1987**, 14–17. (In Chinese)
123. Sun, M.I. Tests and discussions on the critical strength of concrete subjected to freezing. *Low Temp. Archit. Technol.* **1992**, 2–6. (In Chinese)
124. Yang, Y.Z.; Wang, Z.; Gao, X.J.; Ba, H.J. Frozen critical strength and durability of negative temperature concrete. *J. Wuhan Univ. Technol.* **2009**, *31*, 37–41. (In Chinese)
125. *JGJ/T 104-2011*; Winter Construction Regulations for Building Projects. Ministry of Housing and Urban-Rural Development of the People's Republic of China. China Construction Industry Press: Beijing, China, 2011. (In Chinese)
126. Zhu, W.Z.; Gao, Y.B.; Shi, M.X. Influence of one freezing mode on the freezing critical strength of antifreeze concrete. *Low Temp. Constr. Technol.* **1993**, 36–38. (In Chinese)
127. Zhu, W.Z.; Ma, W.H.; Kang, B.Z. Effect of multiple freezing modes on the freezing critical strength of antifreeze concrete. *Low Temp. Archit. Technol.* **1993**, 37–40. (In Chinese)
128. Ma, W.H.; Yu, B.Q. Analysis of the role of antifreeze from the theory of freezing critical strength. *Low Temp. Archit. Technol.* **1995**, 41–42. (In Chinese)
129. Li, J.H.; Wang, Z.; Lu, B.Y. Study on strength development of high strength concrete at negative temperature. *J. Harbin Inst. Technol.* **2002**, 373–375. (In Chinese)
130. Su, X.N.; Wang, X.; Chi, D.C. Experimental study on early freezing of concrete. *Concrete* **2005**, 87–89. (In Chinese)
131. Liu, J.; Li, Z.G.; Tian, Y.; Liu, R.Q. Effects of mineral admixtures on strength development and frost critical strength of concrete under low temperature. *J. Shenyang Jianzhu Univ.* **2006**, *22*, 415–418+427. (In Chinese)



132. Liu, J.; Liu, R.Q. Prediction of antifreeze critical strength of infant age concrete. *J. Wuhan Univ. Technol.-Mater. Sci. Ed.* **2008**, *23*, 272–275. [[CrossRef](#)]
133. Liu, J.; Liu, R.Q. The Antifreeze Critical Strength of Low-temperature Concrete Effected by Index. *J. Wuhan Univ. Technol.-Mater. Sci. Ed.* **2011**, *26*, 354–359. [[CrossRef](#)]
134. An, G.S.; Liu, Z.Y.; Li, J.X. Effect of fly ash on frost critical strength of concrete. *Low Temp. Archit. Technol.* **2016**, *38*, 23–25. (In Chinese)
135. Chen, S.X. Research on the effect of fly ash on the frost critical strength of concrete. *Contemp. Chem. Ind.* **2019**, *48*, 2781–2784. (In Chinese)
136. Liu, Z.Y.; Fu, S.; Ma, G.W.; Wang, S.; Li, B.Y.; Yang, H.; Cui, S.J.; Zhang, Z. Influence of pre-conditioning with electric trace heat on the critical strength of concrete subjected to freezing. *Bull. Chin. Ceram. Soc.* **2022**, *41*, 1990–1997. (In Chinese)
137. Yi, S.T.; Pae, S.W.; Kim, J.K. Minimum curing time prediction of early-age concrete to prevent frost damage. *Constr. Build. Mater.* **2011**, *25*, 1439–1449. [[CrossRef](#)]
138. Liu, D.Y.; Tu, Y.M.; Shi, P.; Sas, G. Mechanical and durability properties of concrete subjected to early-age freeze–thaw cycles. *Mater. Struct.* **2021**, *54*, 211. [[CrossRef](#)]
139. Li, Y.; Chai, J.Q.; Wang, R.J.; Zahng, X. Experimental evaluation of the frost resistance durability of RCC layer subjected to early-age freezing. *J. Build. Eng.* **2023**, *76*, 107153. [[CrossRef](#)]

**Disclaimer/Publisher’s Note:** The statements, opinions and data contained in all publications are solely those of the individual author(s) and contributor(s) and not of MDPI and/or the editor(s). MDPI and/or the editor(s) disclaim responsibility for any injury to people or property resulting from any ideas, methods, instructions or products referred to in the content.